JVP
Journal of Vertebrate Paleontology

SVP
SOCIETY OF VERTEBRATE PALEONTOLOGY

Volume 31, Number 3
May 2011

Featured Article:

Cranial osteology of a juvenile specimen of *Tarbosaurus bataar* (Theropoda, Tyrannosauridae) from the Nemegt Formation (Upper Cretaceous) of Bugin Tsav, Mongolia

Print ISSN 0272-4634
Online ISSN 1937-2809

Journal of Vertebrate Paleontology 31(3):497–517, May 2011

FEATURED ARTICLE

CRANIAL OSTEOLOGY OF A JUVENILE SPECIMEN OF *TARBOSAURUS BATAAR* (THEROPODA, TYRANNOSAURIDAE) FROM THE NEMEGT FORMATION (UPPER CRETACEOUS) OF BUGIN TSAV, MONGOLIA

TAKANOBU TSUIHIJI,[*,1] MAHITO WATABE,[2] KHISHIGJAV TSOGTBAATAR,[3] TAKEHISA TSUBAMOTO,[2] RINCHEN BARSBOLD,[3] SHIGERU SUZUKI,[2] ANDREW H. LEE,[4,†] RYAN C. RIDGELY,[4] YASUHIRO KAWAHARA,[2] and LAWRENCE M. WITMER[4]

[1]Department of Geology and Paleontology, National Museum of Nature and Science, 3-23-1 Hyakunin-cho, Shinjuku-ku, Tokyo 169-0073, Japan, taka@kahaku.go.jp;
[2]Center for Paleobiological Research, Hayashibara Biochemical Laboratories, Inc., 1-2-3 Shimoishii, Okayama 700–0907, Japan;
[3]Mongolian Paleontological Center, Mongolian Academy of Sciences, Enkh Taivan Street-63, Ulaanbaatar 210351, Mongolia;
[4]Department of Biomedical Sciences, College of Osteopathic Medicine, Ohio University, Athens, Ohio 45701, U.S.A.

ABSTRACT—A juvenile skull of the tyrannosaurid *Tarbosaurus bataar* found in the Bugin Tsav locality in the Mongolian Gobi Desert is described. With a total length of 290 mm, the present specimen represents one of the smallest skulls known for this species. Not surprisingly, it shows various characteristics common to juvenile tyrannosaurids, such as the rostral margin of the maxillary fenestra not reaching that of the external antorbital fenestra and the postorbital lacking the cornual process. The nasal bears a small lacrimal process, which disappears in adults. Lacking some of the morphological characteristics that are adapted for bearing great feeding forces in adult individuals, this juvenile specimen suggests that *T. bataar* would have changed its dietary niches during ontogeny. The numbers of alveoli in the maxilla (13) and dentary (14 and 15) are the same as those in adults, suggesting that they do not change ontogenetically in *T. bataar* and thus are not consistent with the hypothesis that the numbers of alveoli decreases ontogenetically in tyrannosaurids.

INTRODUCTION

The tyrannosaurid *Tarbosaurus bataar* (Maleev, 1955a) from the Upper Cretaceous Nemegt Formation of the Gobi Desert is known from numerous specimens (Hurum and Sabath, 2003), and its anatomy has been extensively studied (e.g., Maleev, 1965, 1974; Hurum and Currie, 2000; Hurum and Sabath, 2003; Saveliev and Alifanov, 2007). These studies, however, were based mostly on adult or subadult specimens, and juvenile individuals of this dinosaur have rarely been found or described, unlike North American tyrannosaurids such as *Albertosaurus*, *Daspletosaurus*, and *Tyrannosaurus* for which immature individuals and even growth series are known (Carr, 1999, 2010; Currie, 2003a; Carr and Williamson, 2004). One exception is the holotype specimen of "*Shanshanosaurus huoyanshanensis*" from northwestern China (Dong, 1977), which Currie and Dong (2001) and Currie (2003b) suggested might pertain to a juvenile *T. bataar*. However, while preserving a fair number of postcranial bones, especially the presacral vertebral series, the specimen of "*S. huoyanshanensis*" lacks most of the cranial bones except for the right maxilla and lower jaw (Dong, 1977; Currie and Dong, 2001). Thus, ontogenetic changes in the cranial morphology in *T. bataar* remain largely unknown.

During the Hayashibara Museum of Natural Sciences–Mongolian Paleontological Center Joint Expedition in the western Gobi Desert in 2006, an articulated, juvenile skeleton of *T. bataar* was collected at the Bugin (Bügiin) Tsav locality, where larger, adult specimens of this dinosaur have also been collected (e.g., Barsbold, 1974, 1983; Suzuki and Watabe, 2000; Watabe and Suzuki, 2000a, 2000b). This juvenile specimen, cataloged as MPC-D 107/7 in the Mongolian Paleontological Center, Mongolian Academy of Sciences, lacks parts of the vertebral column and associated ribs or chevrons (i.e., the entire cervical and cranial dorsal series and distal four fifths of the caudal series), but preserves almost all other bones (Fig. 1A, B). Most remarkably, MPC-D 107/7 includes an articulated skull (Figs. 1C, 2–4, 5A–E), which is especially well preserved on the left side where only the articular is missing. In the present paper, we describe the morphology of this skull with an emphasis on ontogenetically variable characteristics. An analysis of included soft tissues (e.g., brain, inner ear, sinuses) along with a restoration of the skull and a description of the postcranial anatomy of this specimen will be published elsewhere.

MATERIALS AND METHODS

Institutional Abbreviations—**BMR**, Burpee Museum of Natural History, Rockford, Illinois, U.S.A.; **CMNH**, Cleveland Museum of Natural History, Cleveland, Ohio, U.S.A.; **GIN**, Institute of Geology, Ulaanbaatar, Mongolia; **LACM**, Natural History Museum of Los Angeles County, Los Angeles, California, U.S.A.; **MPC**, Mongolian Paleontological Center, Ulaanbaatar, Mongolia; **ZPAL**, Institute of Palaeobiology, Warszawa, Poland.

Anatomical Abbreviations—**?III**, possible foramen for the oculomotor nerve; **V_1**, foramen for the ophthalmic branch of the trigeminal nerve; **V_{2-3}**, foramen for the maxillary and mandibular branches of the trigeminal nerve; **VII**, foramen for the facial nerve; **A**, angular; **aj**, **aq**, and **as**, articular surfaces of the quadratojugal for the jugal, quadrate, and squamosal, respectively;

*Corresponding author. †Current address: Department of Anatomy, Midwestern University, 19555 N. 59th Ave., Glendale, Arizona 85308, U.S.A.

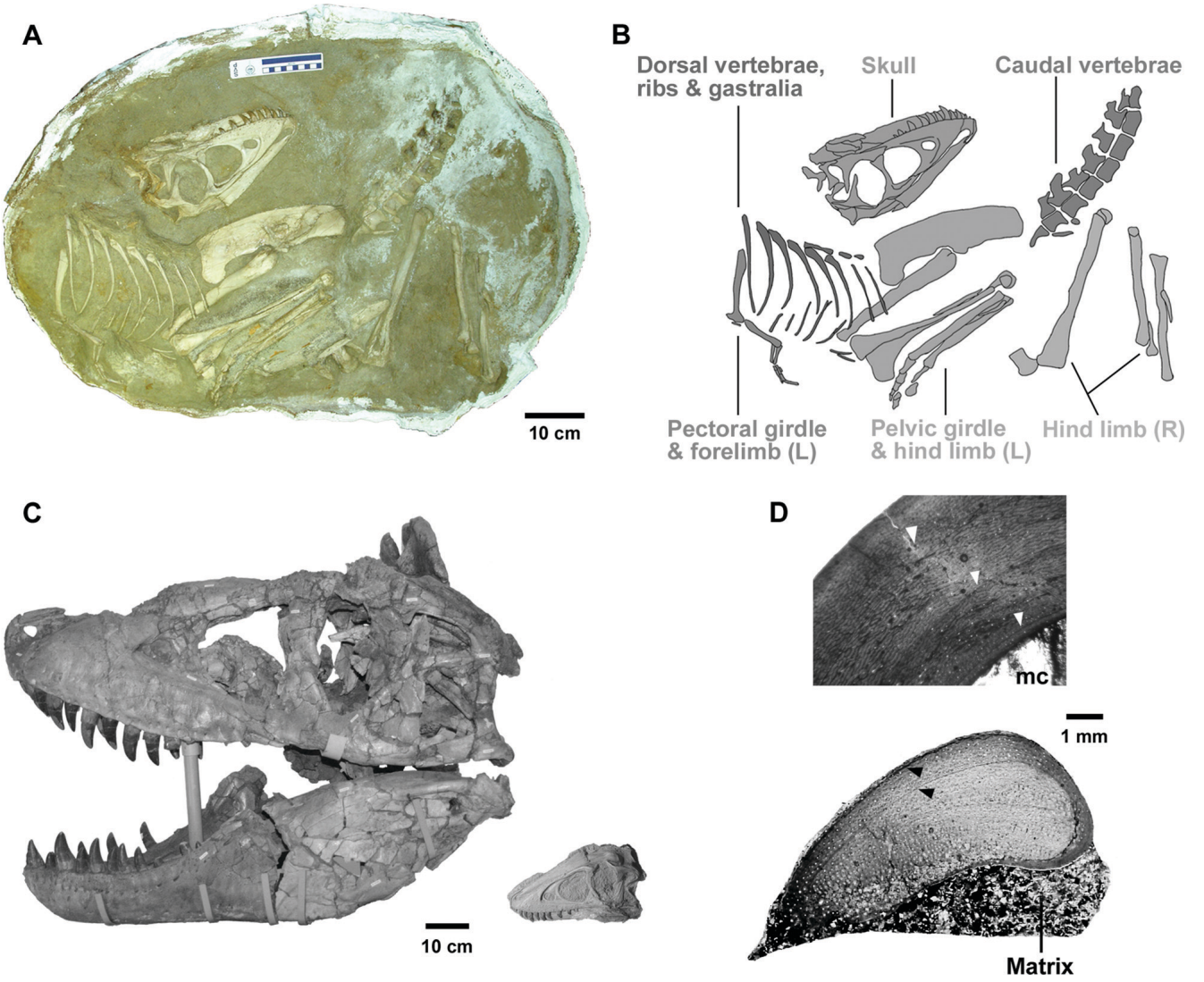

FIGURE 1. Juvenile *Tarbosaurus bataar* (MPC-D 107/7). **A**, photograph of the specimen prior to complete preparation, and **B**, its interpretative drawing. **C**, skull (right) compared with that of a large adult (MPC-D 107/2, left, reversed) in the same scale; **D**, histological thin sections of the left tibia (above) and fibula (below) made at mid-diaphysis. Arrowheads indicate lines of arrested growth. (Figure appears in color online.).

aoc, antotic crest; **apo**, articular surface of the jugal for the postorbital; **BS**, basisphenoid; **bsr**, basisphenoid recess; **c** and **r**, grooves marking courses of the caudal and rostral rami of the facial nerve, respectively; **cap**, capitate process of the laterosphenoid; **cor**, columellar recess; **cp**, cornual process; **csf**, caudal surangular foramen; **ctr**, caudal tympanic recess; **cup**, cultriform process; **D**, dentary; **da**, depression representing the jugal part of the antorbital fossa; **dpaM** and **vpaM**, dorsal and ventral prongs of the ascending ramus of the maxilla, respectively; **ECT**, ectopterygoid; **EPP**, epipterygoid; **F**, frontal; **iaofe**, internal antorbital fenestra; **J**, jugal; **L**, bones on the left side; **LA**, lacrimal; **llr** and **mlr**, lateral and medial laminae of the rostral ramus of the lacrimal, respectively; **lpr**, lacrimal pneumatic recess; **lr**, aperture of the lacrimal recess; **LS**, laterosphenoid; **M**, maxilla; **mc**, medullary cavity; **mf**, maxillary fenestra; **N**, nasal; **nlc**, groove continuing rostrally from the nasolacrimal canal; **OO**, otoccipital; **osc**, otosphenoidal crest; **P**, parietal; **PA**, palatine; **paroc**, paroccipital process; **pe**, pneumatic excavation; **PF**, prefrontal; **pf**, pituitary fossa; **pfp**, pneumatic fossae on the palatine; **PM**, premaxilla; **pmf**, promaxillary fenestra; **PO**, postorbital; **pqf**, paraquadrate foramen; **PRA**, prearticular; **PRO**, prootic; **prp**, preotic pendant; **PS**, parasphenoid; **PT**, pterygoid; **Q**, quadrate; **QJ**, quadratojugal; **R**, bones on the right side; **rtr**, rostral tympanic recess; **S**, squamosal; **SA**, surangular; **scf**, subcutaneous flange; **SCL**, sclerotic ring; **SE**, sphenethmoid; **snf**, subnarial foramen; **SO**, supraoccipital; **sop**, suborbital process; **SPL**, splenial; **stf**, postorbital part of the supratemporal fossa; **t**, tubercle; **V**, vomer.

Comparative Materials—Skulls of two cataloged specimens of *Tarbosaurus bataar*, MPC-D 107/2 and 107/14, were observed for comparison with MPC-D 107/7. MPC-D 107/2 is a large adult skeleton, of which the articulated skull is 122 cm in rostrocaudal length (Currie and Carpenter, 2000). This specimen was formerly known as GIN 107/2 in the scientific literature (e.g., Currie and Carpenter, 2000; Currie, 2003a; Hurum and Sabath, 2003). The acronym of this specimen (as well as of all other specimens formerly housed in the GIN) has been changed to MPC after establishment of the Mongolian Paleontological Center in 1996. MPC-D 107/14 includes several disarticulated cranial and postcranial

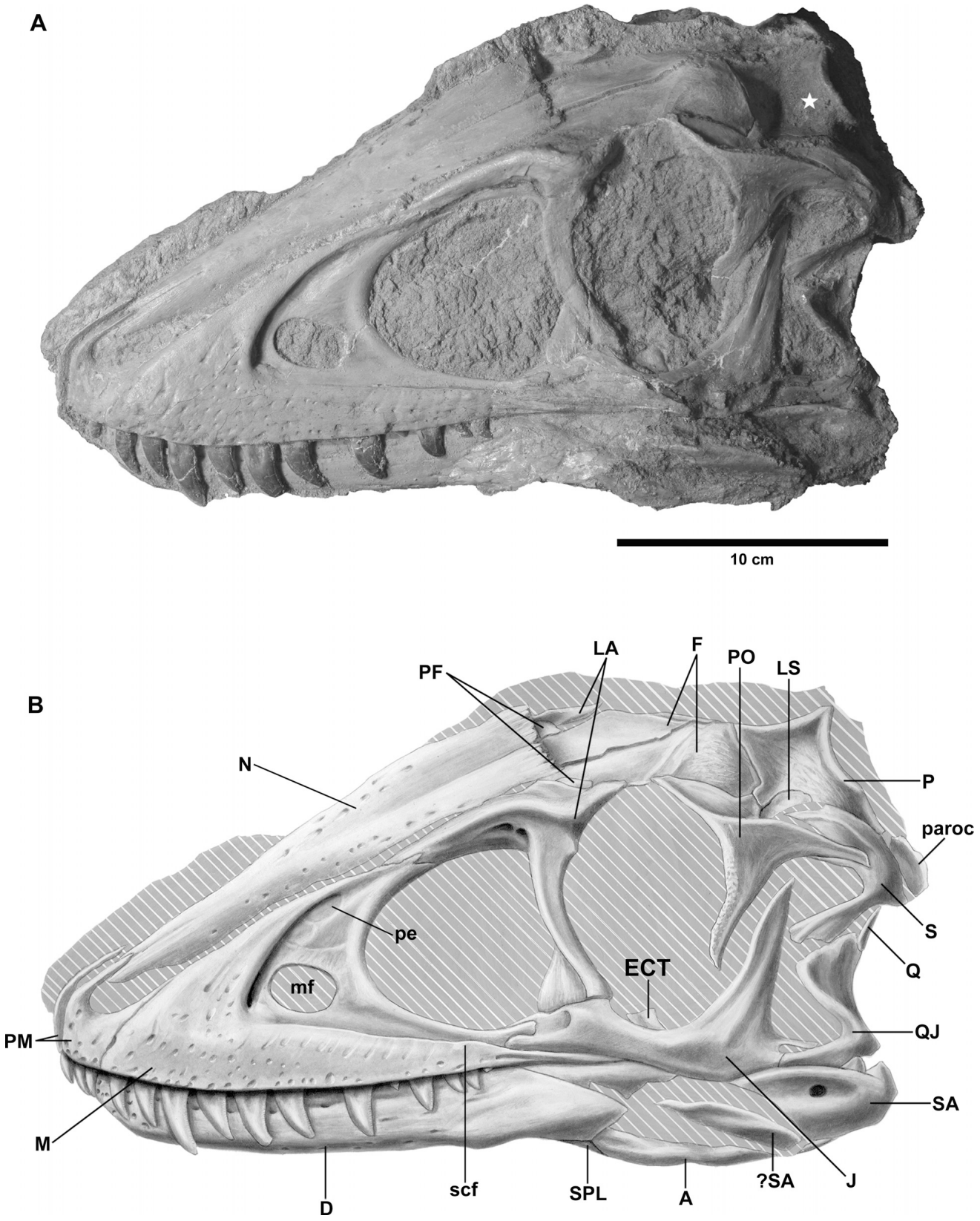

FIGURE 2. Skull of a juvenile *Tarbosaurus bataar* (MPC-D 107/7) in left lateral view. **A**, photograph; **B**, drawing. In **A**, the caudal part of the left supratemporal fenestra is still covered by matrix (indicated by a white star).

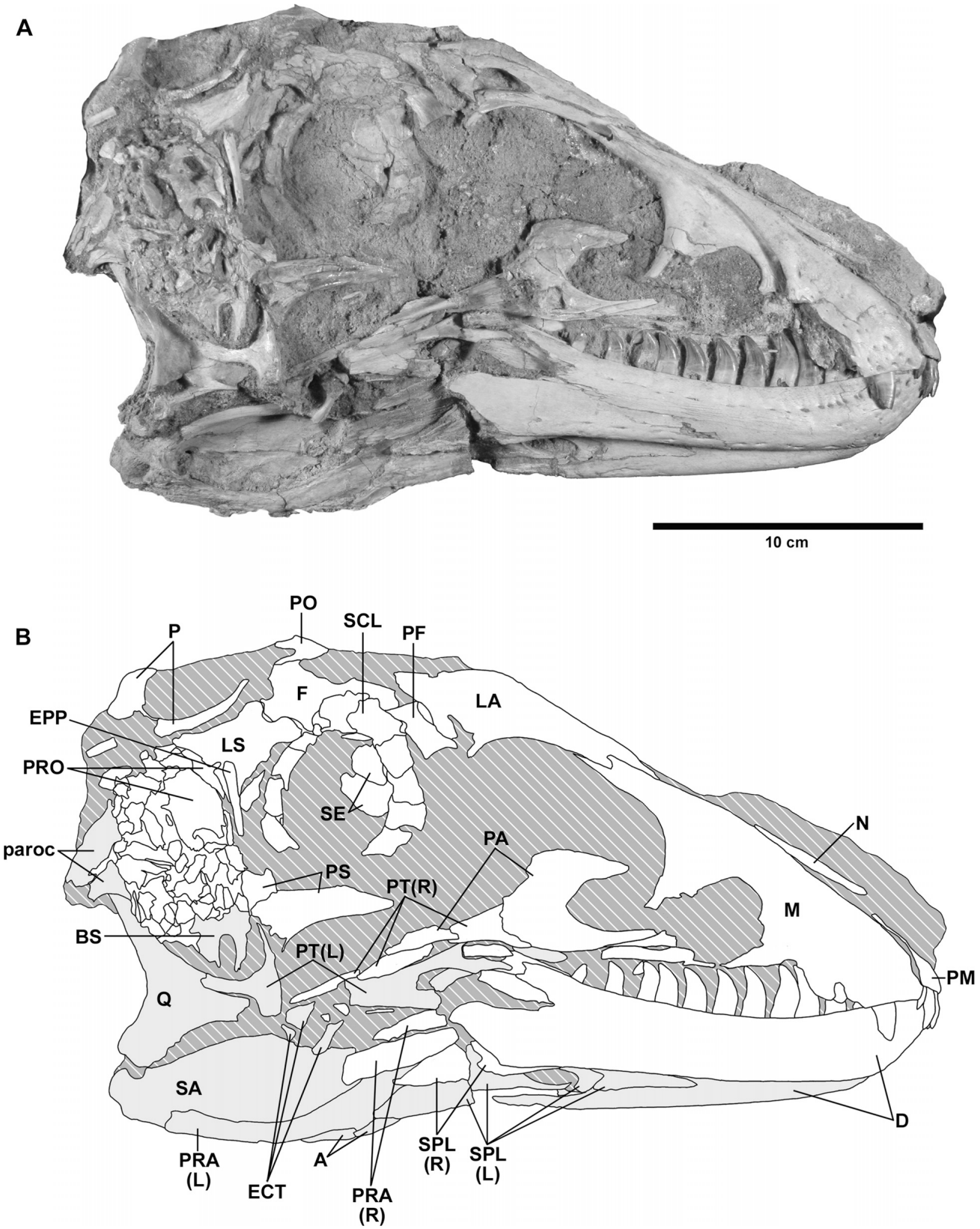

FIGURE 3. Skull of a juvenile *Tarbosaurus bataar* (MPC-D 107/7) in right lateral view. **A**, photograph; **B**, interpretative drawing showing bones on the right and left sides in white and grey in color, respectively.

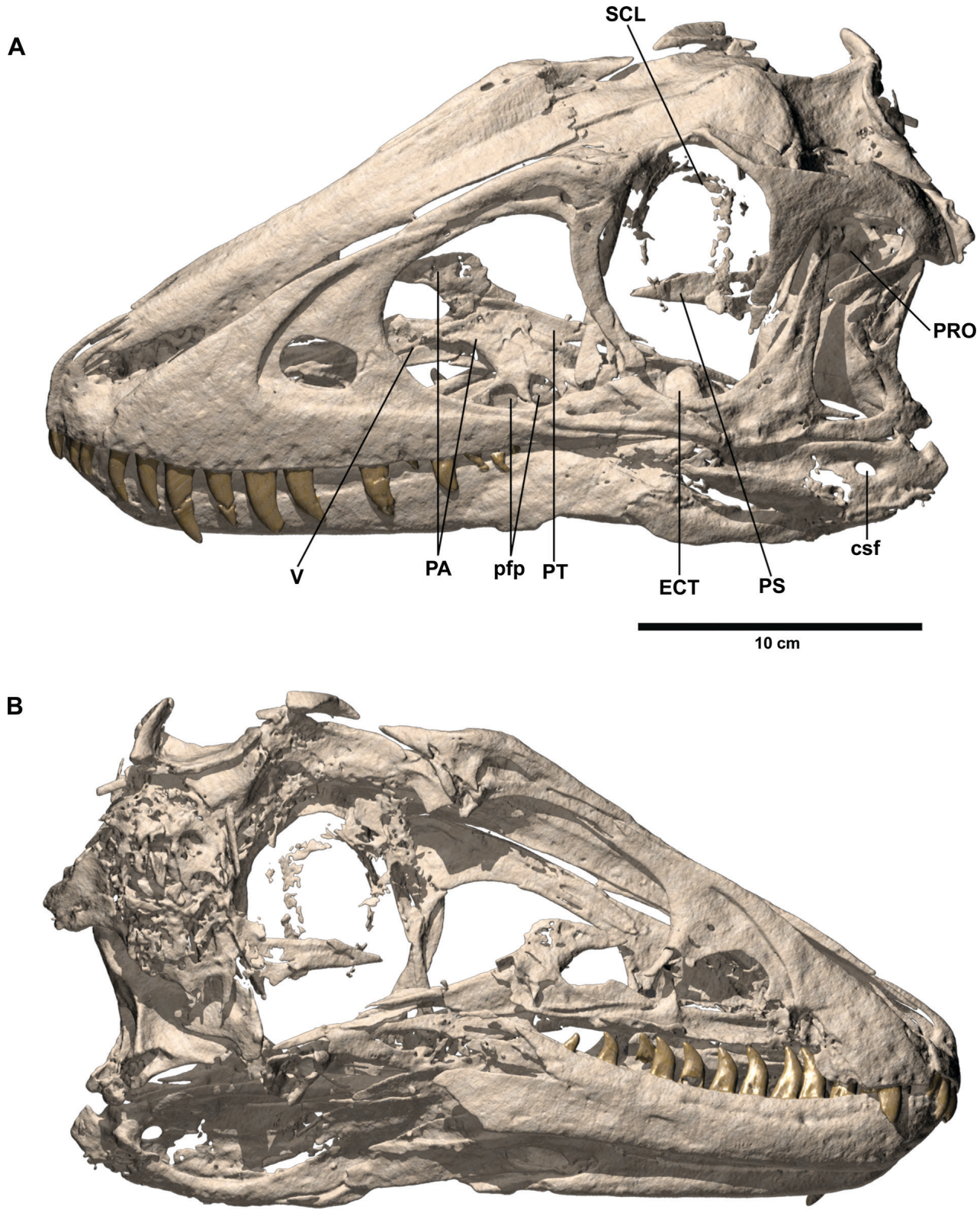

FIGURE 4. Surface rendering images of the skull of a juvenile *Tarbosaurus bataar* (MPC-D 107/7) based on the CT data with the matrix digitally removed. **A**, left lateral view; **B**, right lateral view. Bones that are largely concealed within matrix in Figures 2 and 3 are identified in this figure. (Figure appears in color online.).

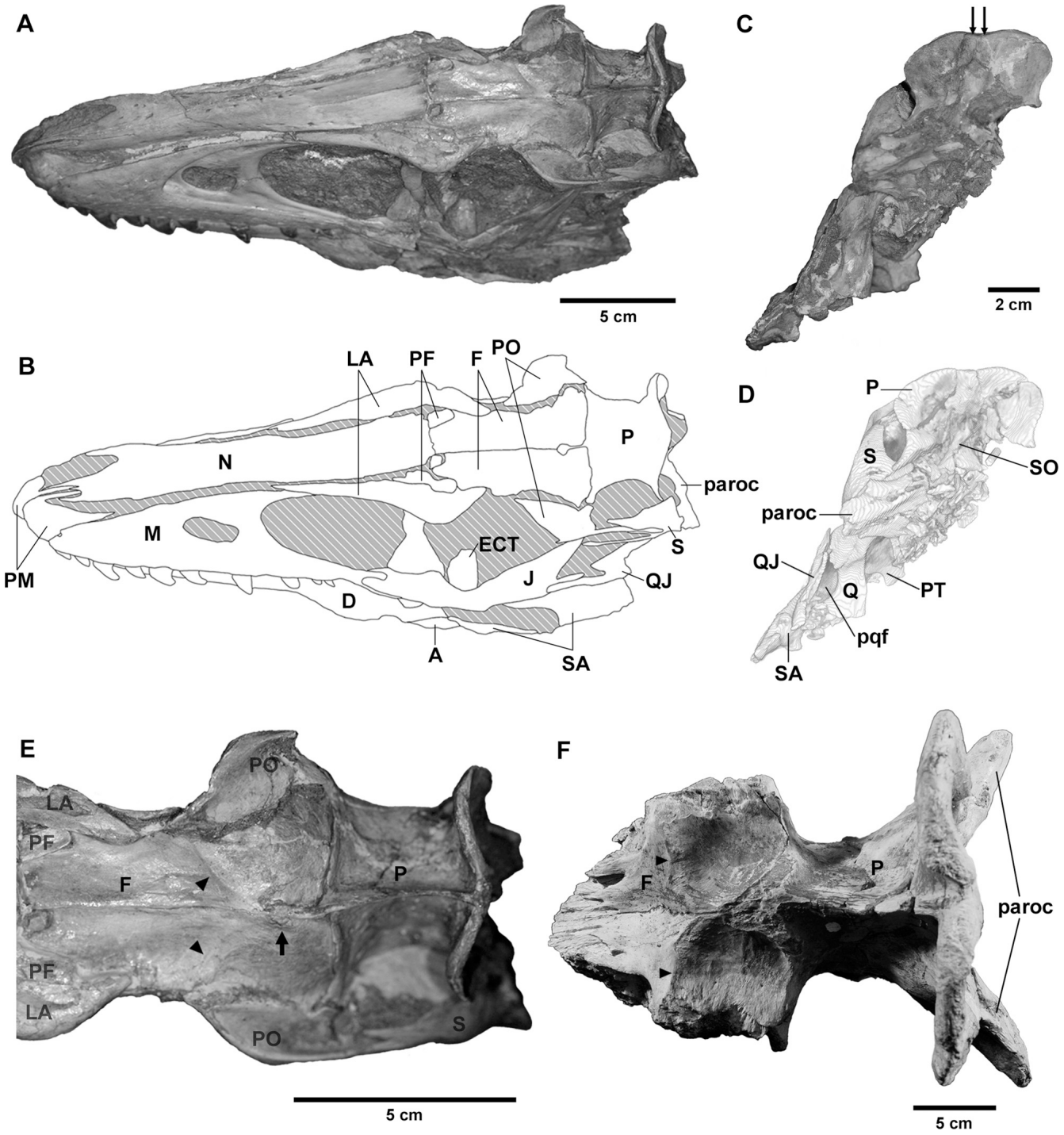

FIGURE 5. Skull of a juvenile *Tarbosaurus bataar* (MPC-D 107/7). **A** and **B**, photograph and interpretative drawing, respectively, in dorsal view; **C** and **D**, photograph and volume rendering image based on the CT data, respectively, in caudal view; **E** and **F**, close-up of the frontal and parietal (**E**) in comparison with those of a larger individual (MPC-D 107/14, **F**) in dorsal view. The arrow in **E** indicates a mushroom-like rostral process of the parietal invading between the right and left frontals. Arrowheads in **E** and **F** indicate rostral margins of the supratemporal fossae.

bones of at least three individuals of varying sizes. These individuals probably belong to large juveniles or young adults and are much smaller than MPC-D 107/2.

Computed Tomography Scan—In order to supplement observations on the external surface, the present specimen was subjected to X-ray computed tomographic (CT) imaging. It was scanned helically on a General Electric LightSpeed Ultra Multi-Slice CT scanner at O'Bleness Memorial Hospital, Athens, Ohio, with a slice thickness of 625 μm at 120 kV and 200 mA. Observations on image slices and three-dimensional (3D) visualization were done using the software package Amira 4.1.2 (Visage Imaging Inc., Chelmsford, MA).

GEOLOGICAL SETTING

The Bugin Tsav locality is situated in the western part of the Gobi Desert and has been known as one of the most fossiliferous dinosaur localities in Mongolia (e.g., Barsbold, 1983; Kurochkin and Barsbold, 2000). The Late Cretaceous Nemegt Formation crops out at this locality (e.g., Gradzínski et al., 1977; Shuvalov, 2000), consisting mostly of sediments of a meandering fluvial system (e.g., Suzuki and Watabe, 2000; Weishampel et al., 2008). The age of the Nemegt Formation is not well constrained, with estimates ranging from late Campanian–early Maastrichtian to Maastrichtian (e.g., Gradzínski et al., 1977; Jerzykiewicz and Russell, 1991; Jerzykiewicz, 2000), as reviewed in Weishampel et al. (2008).

SYSTEMATIC PALEONTOLOGY

DINOSAURIA Owen, 1842
THEROPODA Marsh, 1881
COELUROSAURIA Huene, 1914
TYRANNOSAURIDAE Osborn, 1906

TARBOSAURUS BATAAR (Maleev, 1955a)
(Figs. 1–4, 5A–E, 6, 7, 8A, E, G, 9–11)

Material—MPC-D 107/7, articulated, juvenile skeleton missing cervical and cranial dorsal vertebrae and ribs, as well as the distal four fifths of the caudal vertebral series.

Locality—Bugin Tsav, western Gobi Desert, Mongolia.

Formation/Age—Nemegt Formation (late Campanian–early Maastrichtian to Maastrichtian).

DESCRIPTION

Taxonomic Identification of MPC-D 107/7

The tyrannosaurid affinity of MPC-D 107/7 is firmly established based on numerous cranial (e.g., fused nasals, infratemporal fenestra constricted by the squamosal-quadratojugal flange, 'D-shaped' cross-section of the premaxillary teeth) and postcranial (e.g., third metacarpal bearing no phalanges, ilium bearing a prominent, ventral projection from the preacetabular process as well as a vertical crest dorsal to the acetabulum on the lateral surface) synapomorphies of Tyrannosauroidea and Tyrannosauridae observed in the specimen (Holtz, 2001, 2004; Currie et al., 2003). Following Rozhdestvensky (1965), Barsbold (1983), and Currie (2000) among others, we consider that the four tyrannosaurid taxa described by Maleev (1955a, 1955b) belong to a single species, *Tarbosaurus bataar*, which is by far the most common tyrannosaurid in the Nemegt Formation. Other tyrannosaurids known from the Nemegt Formation are *Alioramus remotus* described by Kurzanov (1976) and *Alioramus altai* recently described by Brusatte et al. (2009). Among these taxa, MPC-D 107/7 is considered as belonging to *T. bataar* for the following reasons. Firstly, the Bugin Tsav locality has yielded adult specimens of only *T. bataar* and no other tyrannosaurids. Secondly, the numbers of alveoli in the maxilla and dentary in MPC-D 107/7 are within the range of those of *T. bataar*, which has 12 or 13 teeth in the maxilla and 14 or 15 in the dentary (Maleev, 1974; Currie, 2003a; Hurum and Sabath, 2003). The numbers of alveoli in MPC-D 107/7 (confirmed with the CT scan data) are 13 in the left maxilla and 15 and 14 in the dentaries (Fig. 6A). In contrast, both species of *Alioramus* have more teeth, 16 in the maxilla and 18 in the dentary in *A. remotus* (Kurzanov, 1976) and 17 in the maxilla and 20 in the dentary in *A. altai* (Brusatte et al., 2009), respectively. Thirdly, two features that are considered as characterizing *T. bataar* are observed in MPC-D 107/7. One is the caudal surangular foramen, which is relatively smaller than those in other tyrannosaurids (Holtz, 2004). The other is presence of an incipient subcutaneous flange, which is a ridge that extends along the ventral margin of the external antorbital fossa (Fig. 2) and was identified as a diagnostic character of *T. bataar* by Carr (2005). Fourthly, species of *Alioramus*, especially *A. altai*, are characterized by numerous autapomorphies. Such features include a series of osseous knobs or hornlets on the nasals observed in both *A. remotus* and *A. altai*, and an elongated maxillary fenestra, a laterally projecting horn on the jugal, and pneumatic foramina on dorsal ribs observed in *A. altai* (Brusatte et al., 2009). None of these features are present in MPC-D 107/7, making the assignment of MPC-D 107/7 to *T. bataar* virtually certain.

Estimation of the Age of Death

To assess the age of death of MPC-D 107/7, transverse mid-diaphyseal sections were taken from the left fibula and tibia (Fig. 1D). Both sections preserve similar numbers of lines of arrested growth (LAGs). Two LAGs occur in the section from the fibula. Because the fibular section lacks a medullary cavity and has only minor osteonal remodeling in the medial (ad-tibial) cortex, the sequence of LAGs appears complete with no loss of the early growth record. In contrast, a large medullary cavity occurs in the section from the tibia and suggests a need to retrocalculate the early portion of the growth record lost to the expansion of the medullary cavity (e.g., Horner and Padian, 2004). However, the tibial cortex preserves three LAGs, which is reasonably concordant with the two LAGs preserved in the fibular cortex. To estimate the growth rate of the tibia, the circumferences of the preserved LAGs were fitted to a linear difference equation, which takes into account the dependency between successive LAGs (Cooper et al., 2008:eq. 2.1). Least squares regression reveals that the mean circumferential growth rate of the tibia was 10.3 mm/year and that the neonatal midshaft diameter and circumference of the tibia was about 10 mm and 35 mm, respectively. Together, the data suggest that MPC-D 107/7 was 2 to 3 years old at death and is comparable to the early, slow-growth phase before entering the exponential growth phase on the mass growth curves of North American tyrannosaurids (Erickson et al., 2004).

Description of the Skull

The skull is compressed mediolaterally and slightly sheared dorsoventrally such that the dorsal surface of the frontals and nasal are now visible on the left lateral aspect (Figs. 2, 4A). The specimen was found with the right side exposed at the locality. Accordingly, the left side of the skull is much better preserved than is the right side and is missing only the articular. On the right side, most bones in the orbital and temporal regions are missing or only partially preserved, exposing the lateral aspect of the braincase, of which the caudal and ventral parts are also badly crushed and weathered (Figs. 3, 4B, 10A). Post-dentary bones in the lower jaw are also mostly missing from the right side.

The rostrocaudal length of the skull (measured from the rostral end of the left premaxilla to the caudoventral corner of the quadratojugal) is 290 mm. The skull length of the holotype specimen of "*Shanshanosaurus huoyanshanensis*," putatively representing a juvenile *Tarbosaurus bataar*, was estimated to be 288 mm (Currie, 2003a). Therefore, the skull of the present specimen is about the same size as the holotype of "*S. huoyanshanensis*." Currie (2003b) suggested that in tyrannosaurids the length of the skull grows isometrically with that of the femur, with these two lengths being approximately the same in any individual. The length of the left femur of MPC-D 107/7 is 303 mm, only slightly greater than that of the skull, thus conforming to Currie's (2003b) analysis.

In the following description of cranial bones, we will mainly focus on features observable on the external surface of the specimen, supplemented by the CT data. In each bone, we will mainly concentrate on characteristics observed in MPC-D 107/7 that show ontogenetic differences from those in adult individuals. The morphology of cranial bones of *T. bataar* has been described in

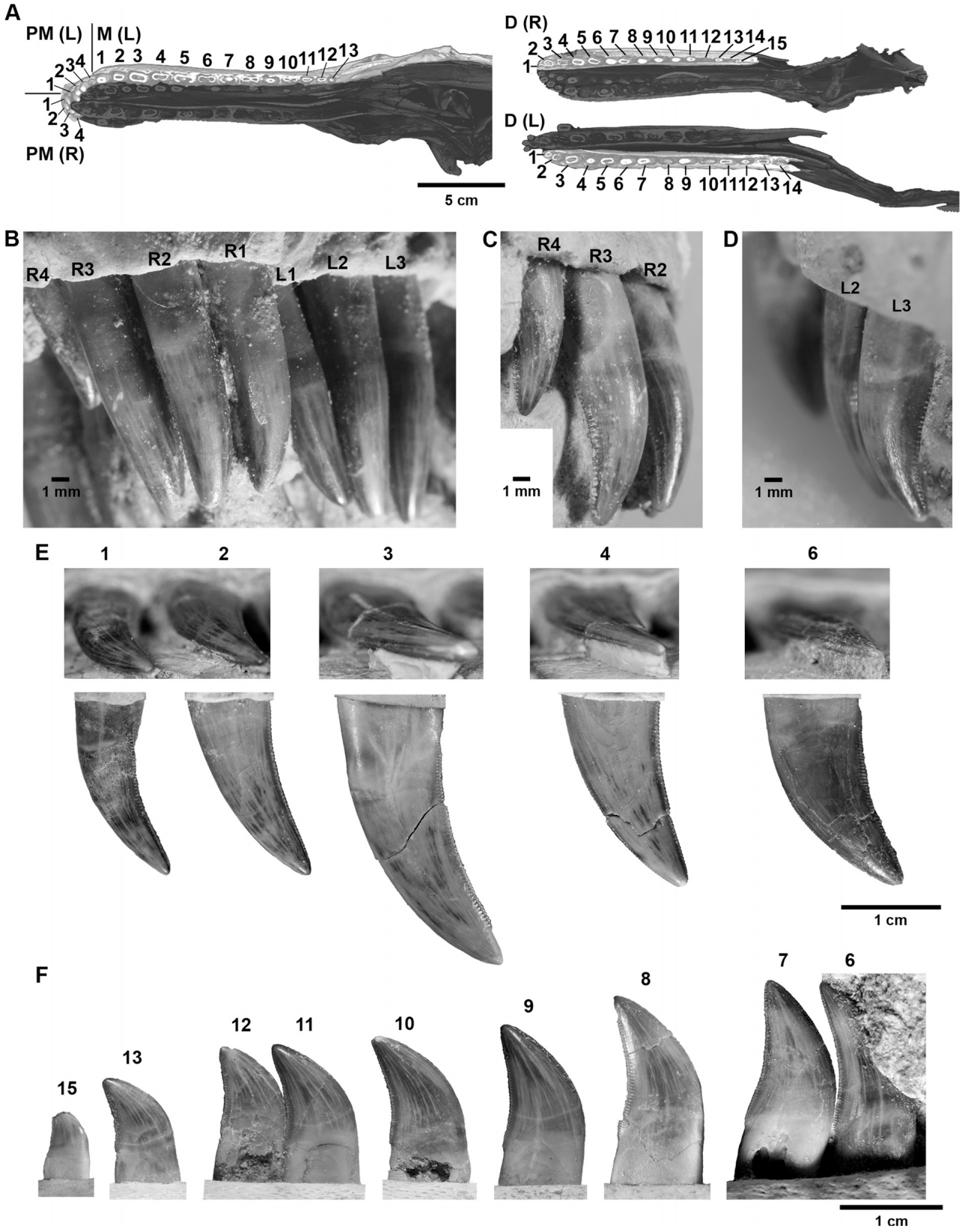

FIGURE 6. Dental morphology of a juvenile *Tarbosaurus bataar* (MPC-D 107/7). **A**, numbers of alveoli counted in frontal sections based on the CT data, with right and left premaxillae and left maxilla in ventral view (left) and right and left dentaries in dorsal view (right). **B**, right and left premaxillary teeth in labial (rostral) view; **C** and **D**, right and left premaxillary teeth in labiodistal view, respectively; **E**, select left maxillary teeth in ventral (above) and labial (below) views; **F**, right dentary teeth in labial view. The numbers indicate the position of each tooth counted from the first (most mesial) alveolus in each bone.

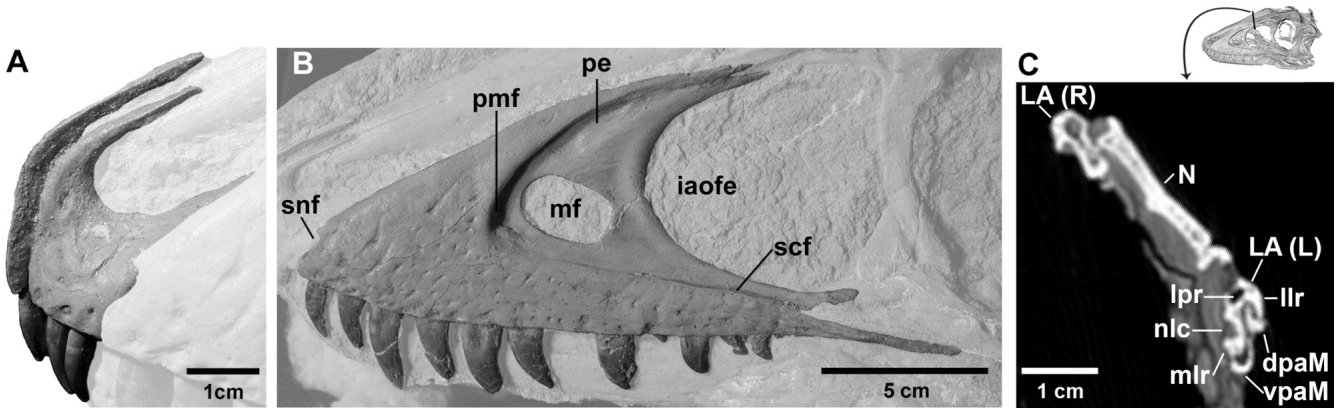

FIGURE 7. Premaxilla and maxilla of a juvenile *Tarbosaurus bataar* (MPC-D 107/7). **A**, left premaxilla in left lateral view, as well as the sutural surface of the right premaxilla in medial view; **B**, left maxilla of MPC-D 107/7 in lateral view; **C**, a transverse section of the rostral skull roof based on the CT data showing the articulation mode between the ascending ramus of the maxilla and the rostral ramus of the lacrimal.

detail by Maleev (1974) and Hurum and Sabath (2003), and these studies serve as a basis for comparison between MPC-D 107/7 and adult conditions. Studies by Carr (e.g., 1999) on craniofacial ontogeny of North American tyrannosaurids serve as the basis for identifying juvenile characteristics in this specimen.

Premaxilla—The body of the premaxilla is relatively narrow mediolaterally in MPC-D 107/7 compared to those in adult specimens (e.g., MPC-D 107/2), which Carr (1999) regarded as a juvenile characteristic in North American tyrannosaurids. In lateral view, it is only slightly deeper dorsoventrally than long rostrocaudally (Fig. 7A). In adult specimens (e.g., MPC-D 107/2), in contrast, its dorsoventral depth is much greater than the rostrocaudal length. The external surface of this premaxillary body is pitted by approximately 10 neurovascular foramina, with the one at the base of the nasal (supranarial) process being the largest. The dorsolateral aspect of the premaxillary body is only shallowly depressed for flooring of the narial tissues, unlike in adults in which this depression (narial fossa) is more pronounced (Hurum and Sabath, 2003; MPC-D 107/2). The nasal process initially projects almost due dorsally from the premaxillary body, and then kinks and extends caudodorsally. Unlike the condition in a juvenile specimen of *Tarbosaurus bataar* mentioned by Currie (2003a), the distal ends of the nasal processes of the right and left premaxillae are appressed to each other and are not forked in MPC-D 107/7. The maxillary (subnarial) process is shaped like a rostrocaudally elongate triangle. It appears to be longer rostrocaudally than in the adult (MPC-D 107/2).

Maxilla—The maxilla of MPC-D 107/7 is dorsoventrally much shallower than in adult specimens (Fig. 7B). For example, the ratio of the maximum height to the maximum length of this bone is 0.39 in this specimen, whereas the same ratio of the specimen described by Hurum and Sabath (2003; ZPAL MgD-I/4, skull length 1100 mm) is 0.57. The main body (alveolar process) of this bone is especially shallow dorsoventrally, representing one of the most prominent juvenile characteristics apparent in this bone. The alveolar margin shows much weaker convexity than in adults, and is almost straight caudal to the fourth alveolus. Caudally, the maxillary body gradually tapers and its caudal end bifurcates into dorsal and ventral processes as in North American tyrannosaurids (Currie, 2003a). The dorsal process forms a part of the medial wall of the antorbital fossa, and extends between two processes at the rostral end of the jugal. The ventral process, the much longer of the two, extends caudally beneath the jugal. The part of the maxillary body rostral to the antorbital fossa appears as a triangle tapering rostrally in lateral view and is low dorsoventrally. At the rostral end, the alveolar and rostrodorsal margins of the bone meet at a more acute angle than in adults. At the premaxillary contact, the rostrodorsal margin is notched for the subnarial foramen, followed caudodorsally by a neurovascular foramen as in adults. The maxillary body is also not thickened laterally, representing an immature condition of tyrannosaurids (Carr, 1999). Although the lateral surface of the maxillary body bears numerous neurovascular foramina and shallow grooves leading to them (for nerves and/or blood vessels), surface sculpturing is not nearly as pronounced as in adults. Four relatively large foramina lie along the rostrodorsal margin of this bone, arranged in a line about 1 cm from the margin. Another row of relatively large foramina extends along the ventral margin of the alveolar process within a few millimeters from the margin, comprising the alveolar row of the foramina of Brochu (2003). As described in *Daspletosaurus* by Carr (1999), a sulcus extends from the caudal-most foramen belonging to this row on the caudal, ventral process described above beneath the jugal in MPC-D 107/7, as in MPC-D 107/2. Brochu's (2003) circumfenestral row of neurovascular foramina, on the other hand, is apparent only in the caudal part of the alveolar process, where neurovascular foramina line up as a straight row along the ventral margin of the external antorbital fenestra.

The margin of the antorbital fossa is well delimited. Unlike in adult specimens such as the one illustrated in Hurum and Sabath (2003) and MPC-D 107/2, this fossa extends caudally beneath the internal antorbital fenestra to extend onto the jugal. That is, the medial wall of this fossa is visible beneath the internal antorbital fenestra in lateral view. The caudal one third of the ventral margin of the antorbital fossa is marked by a sharp ridge representing an incipient subcutaneous flange (Carr, 2005), which becomes less prominent rostrally. At the rostroventral corner of the antorbital fossa, the medial wall of the fossa is slightly laterally convex, or 'swollen' in appearance due to underlying pneumatic sinuses, making the margin of this fossa further obscured. The internal antorbital fenestra, bounded by the maxilla, lacrimal, and jugal, is slightly longer than high (67 mm in length vs. 64 mm in height), whereas it is higher than long in adults (e.g., MPC-D 107/2). The rostral margin of the maxillary fenestra is widely separated from that of the external antorbital fenestra as in the holotype specimen of "*Shanshanosaurus huoyanshanensis*" (Currie and Dong, 2001). This is a conspicuous, juvenile characteristic of tyrannosaurids described by Carr (1999). In adult *Tarbosaurus bataar* (Hurum and Sabath, 2003; MPC-D 107/2), in contrast, the rostral margins of the maxillary fenestra and

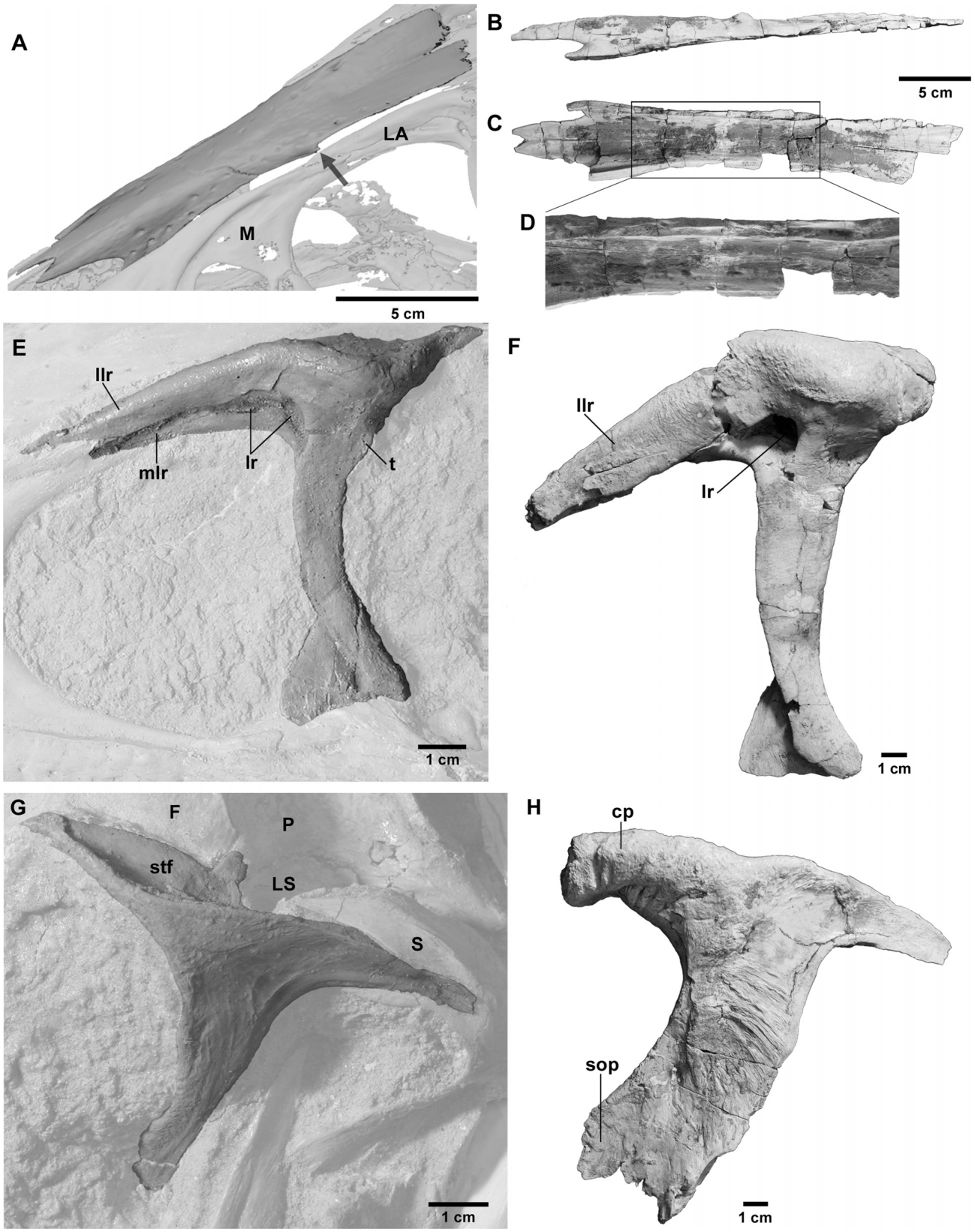

FIGURE 8. Nasal (**A**–**D**), lacrimal (**E**, **F**), and postorbital (**G**, **H**) of *Tarbosaurus bataar*, comparison between a juvenile (MPC-D 107/7) and a larger specimen (MPC-D 107/14). **A**, surface rendering image of the nasals of MPC-D 107/7 based on the CT data in left dorsolateral view, showing the presence of a small lacrimal process on the nasal (arrow), which is lost in larger individuals; **B**–**D**, nasals of MPC-D 107/14 (reversed) in right lateral (**B**), ventral (**C**), and ventrolateral (**D**) views. As shown in **D**, the maxillary contact in MPC-D 107/14 still consists of a longitudinal groove, lacking transverse ridges and grooves observed in fully adult individuals. **E**, left lacrimal of MPC-D 107/7 in lateral view; **F**, right lacrimal of MPC-D 107/14 (reversed) in lateral view. Note that the antorbital fossa is fully exposed laterally on the rostral ramus of the lacrimal in **E**, whereas it is concealed by the lateral lamina of this ramus in **F**. **G**, left postorbital of MPC-D 107/7 in lateral view; **H**, right postorbital of MPC-D 107/14 (reversed) in lateral view.

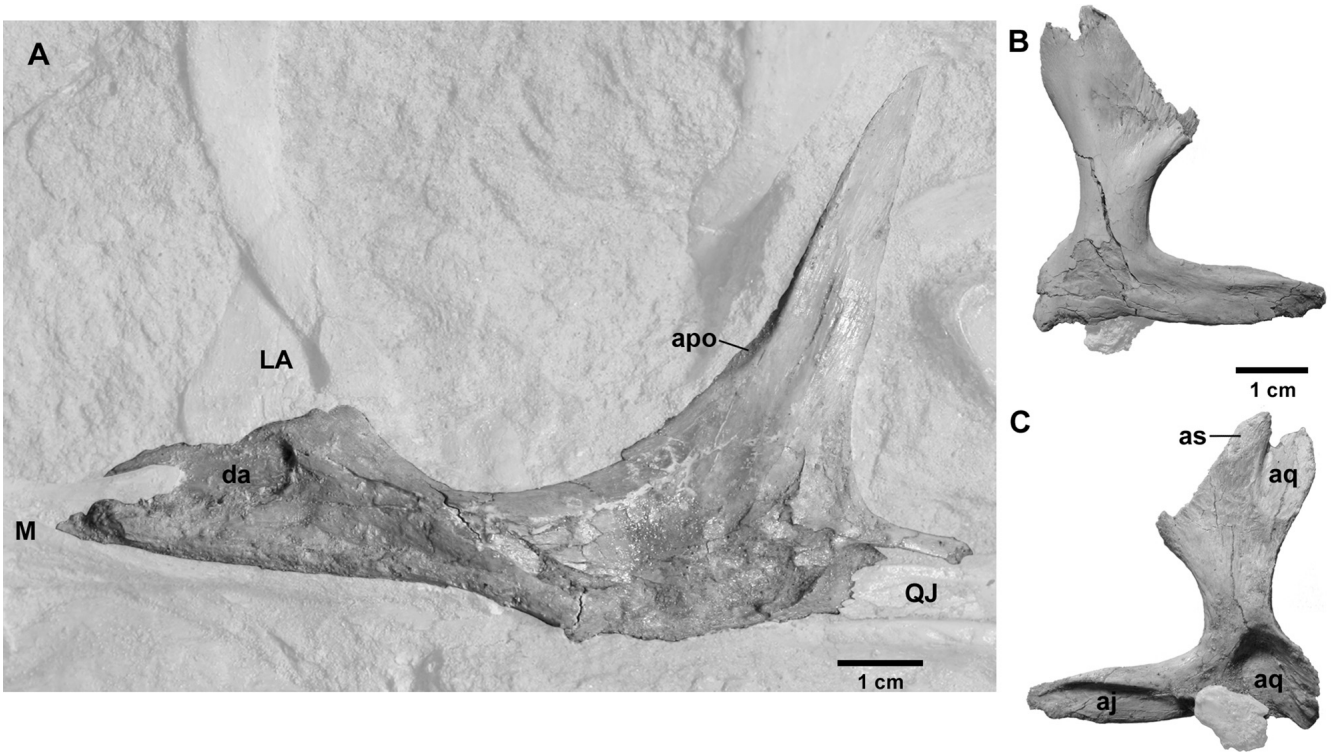

FIGURE 9. Jugal and quadratojugal of a juvenile *Tarbosaurus bataar* (MPC-D 107/7). **A**, left jugal in lateral view; **B** and **C**, right quadratojugal in lateral and medial views, respectively.

external antorbital fenestra approach each other. The maxillary fenestra is clearly longer rostrocaudally than high dorsoventrally (Figs. 2, 7B). Whereas this is still the case in MPC-D 107/2, Hurum and Sabath (2003) described that the height and depth of the maxillary fenestra are the same in the specimen of *T. bataar* that they described. In contrast, Carr (1999) argued that the length-to-height ratio of this fenestra increases ontogenetically in another tyrannosaurid, *Gorgosaurus* (*Albertosaurus*) *libratus*, thus showing an ontogenetic trend possibly opposite to that in *T. bataar*. Dorsal to the maxillary fenestra and along the rostrodorsal margin of the antorbital fossa is an obliquely elongate depression representing a pneumatic excavation (Figs. 2, 7B). The promaxillary fenestra lies at the rostroventral corner of the antorbital fossa, concealed laterally by the rostral rim of the external antorbital fenestra as in the holotype of "*S. huoyanshanensis*" (Currie and Dong, 2001) and most other tyrannosaurid specimens, regardless of age (Witmer, 1997).

The CT scan data revealed that the maxillary sinuses are well developed internally, even at this young age. They basically follow the same pattern as in adult *T. bataar*, *G. libratus*, and *Tyrannosaurus rex* (Witmer, 1997; Hurum and Sabath, 2003; Witmer and Ridgely, 2008). The promaxillary recess is followed caudally by the maxillary antrum, separated from the latter by a vertical bony strut. From the promaxillary fenestra extends a pneumatic excavation forming three interconnected chambers within the ascending ramus (caudodorsal process) of the maxilla. Caudodorsal to the maxillary antrum, a well-developed epiantral recess is present at the junction between the interfenestral strut and pila postantralis. As in other tyrannosaurids (Witmer, 1997; Witmer and Ridgely, 2008), the pila postantralis is not only pneumatic but also fenestrate, allowing the sinus diverticulum within the maxilla to pass caudally to reach the palatine pneumatic chambers.

The ascending ramus of the maxilla tapers caudally and is not particularly massive, unlike the more mature specimen described by Hurum and Sabath (2003). The CT scan data revealed that this process bifurcates into dorsal and ventral prongs at the caudal end and is medially covered by the medial lamina of the rostral ramus of the lacrimal (Fig. 7C). The dorsal prong terminates in a ventrally open trough formed by the medial and lateral laminae of the rostral ramus of the lacrimal. The ventral prong forms a dorsally open trough medially, to which the ventral end of the medial lamina of the lacrimal fits (Fig. 7C).

Nasal—Even at this young age, the right and left nasals are already fused to each other at their mid-length (Figs. 2, 4A, 5A, B, 8A). However, these bones are still separated from each other by a fissure for about one fourth of the length both from the rostral and caudal ends, as in large individuals of *Tarbosaurus bataar* (Maleev, 1974; Hurum and Sabath, 2003). At the rostral end, the nasals are forked along the midline to receive the nasal processes of the premaxillae. The caudal end is apparently broken off and missing from the specimen. The dorsal surface of the fused nasals is still rather smooth, lacking prominent rugosities or papillae, unlike in adult individuals, and bears prominent neurovascular foramina along their lateral margins. Vaulting of these bones is much less pronounced than those in adult individuals such as MPC-D 107/2. The rostral part of the contact surface with the maxilla exposed in right lateral view consists of a shallow, longitudinal groove. The CT scan data revealed the rest of the maxillary articular surface is rather smooth, lacking prominent transverse ridges, or pegs and sockets, unlike the adult condition described by Hurum and Sabath (2003). The maxillary articular surface of the nasals of a larger but still young individual of *T. bataar* (MPC-D 107/14; preserved length of the nasals is 293 mm) also consists of a longitudinal groove, still lacking transverse ridges and grooves (Fig. 8B–D). Such a maxillary articular

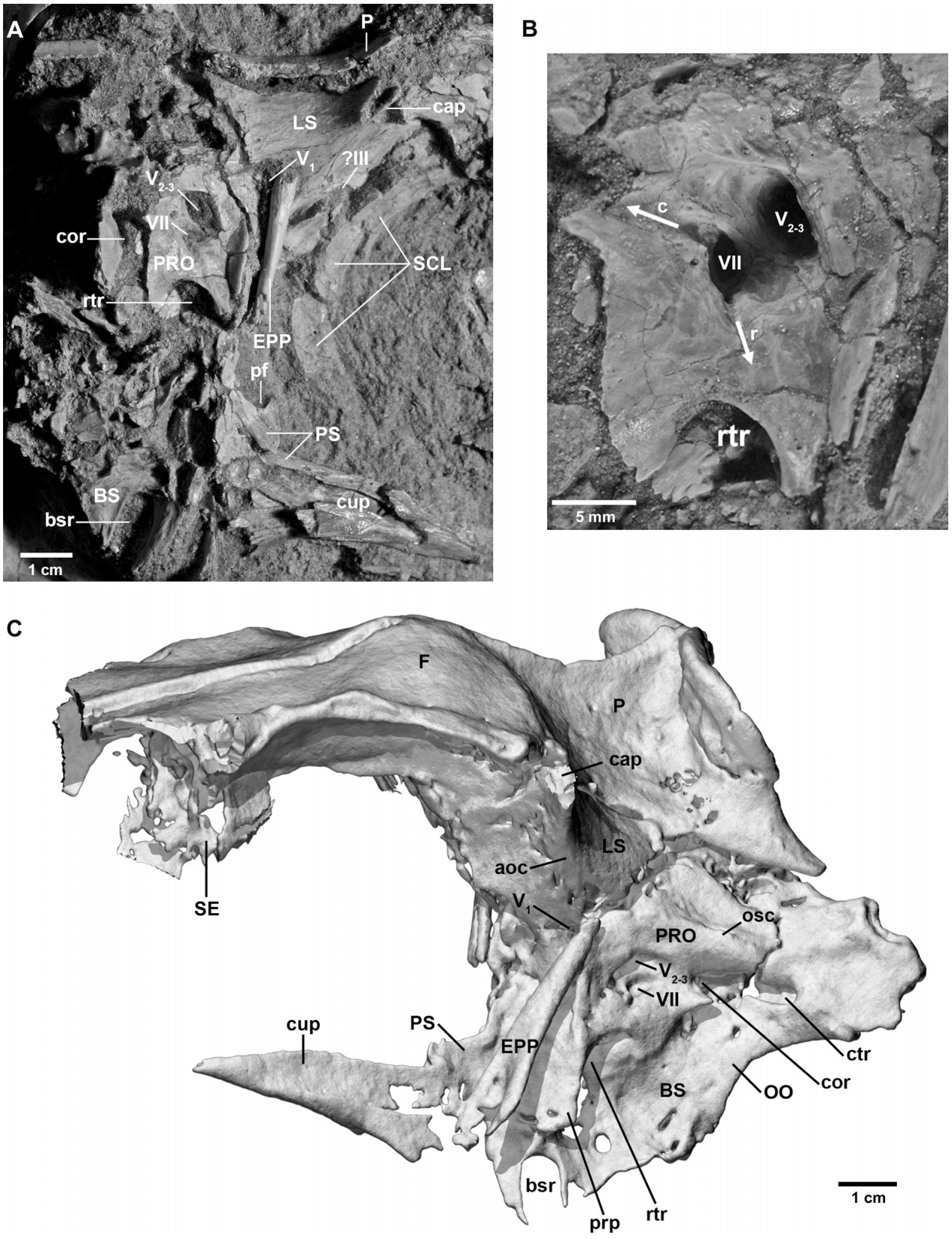

FIGURE 10. Braincase region of a juvenile *Tarbosaurus bataar* (MPC-D 107/7). **A**, photo in right lateral view; **B**, right prootic in lateral view; **C**, surface rendering image based on the CT data in left lateral view.

surface consisting of a longitudinal groove is a general feature seen in young tyrannosaurids (Carr, 1999). The nasal is apparently excluded from the dorsal margin of the external antorbital fenestra in MPC-D 107/7, whereas it forms a part of this margin in adult specimens (e.g., MPC-D 107/2).

The nasal of MPC-D 107/7 has a small lacrimal process (Fig. 8A). Whereas some other tyrannosaurids have this process (e.g., Carr, 1999; Brochu, 2003; Currie, 2003a), Hurum and Sabath (2003) regarded it as lacking in adult *T. bataar*, and Currie et al. (2003) identified its absence (in adults) as a synapomorphy uniting *T. bataar*, *Alioramus remotus*, and *Daspletosaurus*. The presence of such a process, albeit being tiny, in MPC-D 107/7 indicates that this is an ontogenetically variable character in *T. bataar*, as in *Daspletosaurus* in which the lacrimal process is present in juveniles but is lost in mature individuals (Currie, 2003a). Caudally, the nasals slightly expand mediolaterally between the lacrimals. The same condition was described for young stages of *G. libratus* by Carr (1999). The same parts become constricted between the lacrimals in adult *T. bataar* (Carr, 1999; also illustrated in Hurum and Sabath, 2003).

Lacrimal—In lateral view, the lacrimal is T-shaped with the caudal ramus extending behind the ventral ramus (Fig. 8E), unlike in adults in which the caudal ramus is inflated and this bone is shaped like a '7' (Carr et al., 2005) or an inverted 'L' (Fig. 8F). As Carr (1999) described in his youngest stage of *Gorgosaurus libratus*, the rostral ramus of the lacrimal is divided into the lateral and medial laminae, with the former situated dorsal to the latter (Fig. 8E). These two laminae are well separated from each other, and the caudodorsal part of the antorbital fossa expands onto the medial lamina. This part of the antorbital fossa is fully exposed in lateral view (i.e., not hidden by the lateral lamina of the rostral ramus extending ventrally). Such lateral exposure of the entire lacrimal antorbital fossa was identified as an immature feature in *G. libratus* by Carr (1999). Also as in immature, North American tyrannosaurids (Carr, 1999), the caudal end of this fossa is sharply bounded by the rostral edge of the ventral ramus of this bone. In larger specimens of *Tarbosaurus bataar* (e.g., MPC-D 107/14; dorsoventral height of the lacrimal is 172 mm), the rostral part of the antorbital fossa on the rostral ramus appears to be separated from its caudal part bearing the aperture of the lacrimal recess and is concealed in lateral view by the ventrally expanded lateral lamina (Fig. 8F). In an even larger individual (MPC-D 107/2), the lacrimal antorbital fossa almost completely disappears except for a deep lacrimal recess.

The apertures of the lacrimal recess open at the caudodorsal corner of the antorbital fossa between the rostral and ventral rami of the lacrimal. The CT scan data show that the lacrimal recess hollows out the dorsal part of the bone as in *Tyrannosaurus rex* (Brochu, 2003; Witmer and Ridgely, 2008) and extends rostrally within the lateral lamina of the rostral ramus (Fig. 7C). The nasolacrimal canal extends rostrally ventral to the lacrimal recess. The canal opens via a single aperture in the orbit caudally, and then extends rostrally within the medial lamina of the rostral ramus of the lacrimal to open medially into the nasal cavity near the contact with the maxilla (Fig. 7C). This morphology conforms to the basic pattern observed in other theropods (Sampson and Witmer, 2007).

The dorsal margins of the rostral and caudal rami of the lacrimal lack pronounced rugosity (Fig. 8E), unlike in adults (Hurum and Sabath, 2003; MPC-D 107/2). Where the rostral, caudal, and ventral rami meet, the dorsal margin of the bone shows a sinuous curvature, with the rostral part of the caudal ramus plunging ventrally. The caudal ramus, articulating with the frontal, tapers caudally (Fig. 8E) and does not have an inflated appearance, unlike in larger specimens (Hurum and Sabath, 2003; MPC-D 107/2 and 107/14; Fig. 8F). It does not contact the postorbital caudally so that the frontal intervenes between the two to reach the orbital margin (Figs. 2, 5A, B, E). The ventral ramus is relatively thinner rostrocaudally than in larger specimens, and bears a small tubercle near the dorsal end of the caudal margin (Fig. 8E). This tubercle appears to correspond to the one identified as the attachment of the suborbital ligament in *Appalachiosaurus montgomeriensis* by Carr et al. (2005), although its position in MPC-D 107/7 seems too dorsally placed for an attachment of such a ligament that marks the ventrolateral boundary of the orbit, particularly in such a young animal that would have had a relatively large eyeball.

Postorbital—All three rami (rostral, caudal, and ventral rami) are much slenderer in MPC-D 107/7 than those in larger individuals (Fig. 8G, H). The most prominent ontogenetic change is observed in the ventral (jugal) ramus, which becomes much wider rostrocaudally as individuals grow. This rostrocaudal expansion of the ventral ramus makes the relative lengths of the rostral (frontal) and caudal (squamosal or intertemporal) rami appear shorter in larger individuals (Fig. 8H). Unlike in larger specimens (Maleev, 1974; Hurum and Sabath, 2003; MPC-D 107/2 and 107/14), the ventral ramus in MPC-D 107/7 does not bear a rostrally extending suborbital process (Fig. 8G). Instead, it only has a slight rostral expansion bearing a scar on its lateral aspect. Distal to this expansion, the ventral ramus tapers ventrally. The orbit, therefore, is not constricted at its mid-height, unlike in adults. In lateral view, the rostral ramus tapers quickly rostrally and has no cornual process on the caudodorsal margin of the orbit, bearing only weak rugosity (Fig. 8G). The cornual process appears and becomes progressively prominent in larger individual. In MPC-D 107/2, for example, it is massively developed, bearing bony papillae. In dorsal view, the rostral ramus is narrow mediolaterally and its lateral margin meets that of the caudal ramus at an obtuse angle in MPC-D 107/7 (Fig. 5E). In other words, the rostral ramus extends rostromedially with very gentle curvature. In MPC-D 107/2, in contrast, these two rami meet at almost a right angle in dorsal view, with the rostral ramus appearing to extend due medially. In MPC-D 107/7, the lateral and rostrolateral boundaries of the supratemporal fossa are sharply delimited by a ridge along the dorsal margin of the postorbital. This part of the fossa on the rostral ramus of the postorbital is rather shallow, with the articular processes for the frontal and parietal forming the floor of this fossa (Fig. 8G). The CT data revealed that the frontal articular process is dorsoventrally much thinner than in larger individuals (e.g., MPC-D 107/14). The parietal articular process is tab-like, extends further medially than the frontal articular process (Fig. 8G), and is followed ventrally by the articular surface for the laterosphenoid.

Jugal—The rostral (maxillary) ramus and the suborbital part between the rostral and postorbital (ascending) rami are dorsoventrally shallower in MPC-D 107/7 (Fig. 9A) than in larger individuals (Maleev, 1974; Hurum and Sabath, 2003; MPC-D 107/2). The latter part is also relatively longer rostrocaudally than in more mature specimens. These features were identified as immature characteristics in *Gorgosaurus libratus* by Carr (1999). The lacrimal articulates with the dorsal aspect of the rostral ramus, and their articular surface appears as a straight, oblique line in lateral view. The rostrodorsal part of the rostral ramus has a shallow but well-demarcated depression, which, together with the rostroventral lamina of the ventral ramus of the lacrimal, forms the caudoventral corner of the antorbital fossa (Figs. 2, 9A). Large individuals of *Tarbosaurus bataar* have a prominent foramen (called the secondary fossa of the jugal foramen in Carr, 1999, pneumatopore in Currie, 2003a, and jugal foramen in Hurum and Sabath, 2003) in this depression (e.g., Maleev, 1974; Hurum and Sabath, 2003). In MPC-D 107/2, a very large adult, the ridge demarcating the antorbital fossa on the jugal is resorbed, making the margin of this deep foramen grade directly into the lateral surface of the rostal ramus. This is similar to the condition in *Daspletosaurus torosus* described by Carr (1999). In MPC-D 107/7, in contrast, this foramen is rudimentary. However, the CT scan data reveal that much of the length of the jugal is pneumatic,

extending into the base of the postorbital ramus and caudally to near the fork of the caudal (quadratojugal) ramus.

The postorbital ramus is slender. The articular surface for the postorbital is apparent, but is much narrower than those in larger individuals (e.g., Hurum and Sabath, 2003). Hurum and Sabath (2003) described that the lateral surface of the main body of the jugal has a shallow depression at the base of the postorbital ramus in adult *T. bataar*. Such a depression is apparently absent in MPC-D 107/7, although the corresponding area is crushed and obscured in this specimen. The cornual process that is present on the ventral margin of this area in adults is very poorly developed, if present at all, in MPC-D 107/7.

Quadratojugal—Both left and right quadratojugals are preserved in MPC-D 107/7. Whereas the left bone is in situ, articulating with adjacent bones, the right bone was found isolated from the rest of the skull, providing detailed information on its morphology (Fig. 9B, C). As in adults, the dorsal (squamosal) and ventral (jugal) rami extend rostrally. The rostral expansion or flaring of the dorsal ramus appears to start more dorsally in MPC-D 107/7 than in a large adult, MPC-D 107/2. In other words, the vertical shaft of this bone between the dorsal and ventral rami appears to be longer in the former than in the latter. The dorsal margin of the dorsal ramus appears to be inclined obliquely, from caudodorsal to rostroventral directions, unlike in adults in which the dorsal margin is almost horizontal (e.g., MPC-D 107/2). The lateral surface of the dorsal ramus is concave as in adults such as MPC-D 107/2. This concavity, however, lacks the pneumatic foramen present in the quadratojugals of two small, Maastrichtian tyrannosaurid specimens from North America, CMNH 7541 and BMR P2002.4.1 (Witmer and Ridgely, 2010). Absence of pneumatic foramina in the quadratojugal characterizes definitive adult specimens of *Tarbosaurus bataar* (e.g., MPC-D 107/2) as well. The isolated, right quadratojugal shows that a notch is present in the caudal part of the dorsal end of the dorsal ramus (Fig. 9B, C), as illustrated in the same bone in a larger individual in Maleev (1974). Medially, this notch marks the rostral end of the articular surface for the quadrate, and the articular surface for the squamosal lies rostral to this notch (Fig. 9C). Another articular surface of the quadrate lies on the medial aspect of the caudoventral corner of this bone. Rostral to this quadrate articular surface, a rostrocaudally elongate facet occupies most of the length of the ventral ramus. This facet is for articulation with the lateral surface of the ventral prong of the forked, caudal ramus of the jugal (Fig. 9C).

Squamosal—In lateral view, the rostroventral (quadratojugal) ramus of the squamosal extends rostroventrally from the quadrate cotyle, rather than extending rostrally and almost due horizontally as in larger individuals (Hurum and Sabath, 2003; MPC-D 107/2), making an oblique contact line with the quadratojugal (Figs. 2, 4A). The CT data revealed that there is a single, large, presumably pneumatic fossa on the internal aspect of the body of this bone as in larger individuals of *Tarbosaurus bataar* (e.g., Hurum and Sabath, 2003; MPC-D 107/14) and other tyrannosaurids in general, although it does not extend into the postquadratic process in MPC-D 107/7 unlike in North American tyrannosaurids (Witmer, 1997; Witmer and Ridgely, 2008). In a very large adult (MPC-D 107/2), a well-developed rugosity covers the dorsal to caudodorsal margins of the rostrodorsal (postorbital) ramus. In MPC-D 107/7, these margins are rather smooth with only weak striations present.

Quadrate—The left quadrate is preserved in articulation with the quadratojugal and squamosal. As in adult *Tarbosaurus bataar* (Hurum and Sabath, 2003) and other tyrannosaurids in general (e.g., Brochu, 2003; Currie, 2003a), a large paraquadrate foramen is formed between the quadrate and quadratojugal (Fig. 5C, D). The pterygoid flange extends rostrally from the body of the quadrate. This flange bears a prominent facet for articulation with the pterygoid on the medial aspect of its rostral part. The mandibular condyle is partially broken with the medial hemicondyle missing. A pneumatic fossa is located at the base of the pterygoid ramus and rostrodorsal to the mandibular condyle as in adult *T. bataar* (Hurum and Sabath, 2003) and other tyrannosaurids (e.g., Molnar, 1991; Brochu, 2003; Currie 2003a). In CT images, this fossa can be observed to open into internal pneumatic chambers in the quadrate body, mandibular condyle, and pterygoid flange.

Prefrontal—A small prefrontal can be recognized as a separate bone on the skull roof, exposed between the lacrimal and frontal (Figs. 2, 5A, B, E). The left prefrontal is crushed and fragmented between the lacrimal and frontal. Only the caudal part of the right prefrontal is exposed on the dorsal surface, overlain by the dislocated nasals rostrally. This bone, however, is well preserved, and the CT data show that it is rostrocaudally elongated and teardrop-shaped in dorsal view. This right prefrontal is slightly dislocated, and its triangular, lacrimal articular surface is exposed caudal to the lacrimal on the right lateral side of the specimen (Fig. 3). This lacrimal articular surface is demarcated by a sharp ridge from a smooth and slightly concave orbital surface of the descending process. The latter process, which is broken halfway through, is wide mediolaterally but is very thin rostrocaudally.

Frontal—The frontal is markedly longer rostrocaudally than wide mediolaterally in MPC-D 107/7, whereas the width-to-length ratio increases in larger individuals of *Tarbosaurus bataar* (Fig. 5E, F). For example, the width-to-length ratio (the width is measured from the midline to the lateral margin of the bone between the articulations with the lacrimal and postorbital, and the length is measured from the most caudal part of the frontoparietal suture to the rostral end of the frontal bone) is 0.23 in MPC-D 107/7, in which the rostrocaudal length of this bone is 91 mm (measured based on the CT data), whereas this ratio is 0.40 in MPC-D 107/14, in which the length of the frontal is 145 mm. The same ontogenetic trend was found in tyrannosaurids in general by Currie (2003a) and was also described for *Tyrannosaurus rex* by Carr (1999) and Carr and Williamson (2004).

The caudal part of the frontal in MPC-D 107/7 is rounded dorsally, and the rostral part of the supratemporal fossa extends onto it. Unlike in larger specimens (e.g., MPC-D 107/2 and 107/14; Fig. 5F), however, this frontal portion of the supratemporal fossa in MPC-D 107/7 is very shallow and is not markedly concave. A very low ridge extending rostrolaterally from the midline marks the rostral margin of this fossa (Fig. 5E). In adult *T. bataar*, the left and right supratemporal fossae meet along the midline to form the frontal sagittal crest (Hurum and Sabath, 2003; Holtz, 2004). MPC-D 107/7 lacks such a crest, and the area between these fossae is gently convex.

In dorsal view, the suture line between the right and left frontals is clearly visible throughout the contact of these bones, unlike in more mature individuals in which this suture is obliterated caudally (Maleev, 1974; Hurum and Sabath, 2003). This suture line appears as a straight, smooth line in MPC-D 107/7 (Fig. 5E), lacking interdigitation seen in larger individuals (e.g., MPC-D 107/14; Fig. 5F) except for the most caudal part. The suture line with the parietal is almost a straight, transverse line, except on the midline, where a mushroom-like rostral process of the parietal invades between the right and left frontals (Fig. 5E). In more mature specimens, in contrast, the median part of the parietals forms wedge-shaped articulation with the frontals as seen in MPC-D 107/14 (Fig. 5F) and MPC-D 107/2. Unlike in larger individuals (Maleev, 1974; Hurum and Sabath, 2003), a small part of the frontal is exposed to the orbital margin between the lacrimal and postorbital in MPC-D107/7 (Figs. 2, 4A, 5A, B, E).

Parietal—The left and right parietals are already fused together (Fig. 5A, B, E). The most prominent juvenile feature seen in the parietal is a very low nuchal crest, which does not extend much dorsally beyond the level of the frontal skull roof (Figs. 2, 4). The median, sagittal crest extends rostrally from the nuchal

crest almost horizontally, with its dorsal margin being slightly concave ventrally in lateral view. The sagittal crest does not extend onto the frontal (Figs. 2, 4A, 5A, E), unlike in large individuals such as the one illustrated in Hurum and Sabath (2003:fig. 17). The nuchal crest is higher than the sagittal crest in larger individuals of *Tarbosaurus bataar* (Hurum and Sabath, 2003; MPC-D 107/2 and 107/14). In MPC-D 107/7, however, the height of the nuchal crest is almost the same as the maximum height of the sagittal crest at its caudal end (Figs. 2, 4).

In larger individuals of *T. bataar*, both nuchal and sagittal crests are higher than those in MPC-D 107/7. This is especially the case with the nuchal crest. Measured from the dorsal margin of the foramen magnum in caudal view, the nuchal crest is approximately 1.5 times as high as the supraoccipital in MPC-D 107/7 (Fig. 5C, D), but is more than twice as high as the latter in MPC-D 107/2, a large adult. An ontogenetic increase in the height of the nuchal crest was also reported in North American tyrannosaurids by Carr (1999).

In caudal view, the dorsal part of the nuchal crest expands laterally only slightly in MPC-D 107/7 (Fig. 5C, D). In larger individuals, in contrast, the lateral expansion of this crest is pronounced (e.g., Hurum and Sabath, 2003; MPC-D 107/14). The dorsal margin of this crest, which is marked by strong rugosities in adults (e.g., MPC-D 107/2), is rather smooth with only faint scarring present. However, a pair of scars along the midline representing the fleshly insertion of m. spinalis capitis (Tsuihiji, 2010) is already apparent (Fig. 5C).

Other Bones of the Braincase—Although the lateral surface of the braincase is exposed on the right side of the specimen (Figs. 3, 4B, 10A), the morphology of bones of the braincase on this side, except for the prootic (Fig. 10B), laterosphenoid, and part of the parasphenoid, has mostly been obscured due to weathering and crushing. The left side of the braincase, in contrast, is embedded in matrix, but is mostly preserved except for the ventral part of the basisphenoid as revealed by the CT scan data (Fig. 10C). Notable features of these bones of the braincase are described here.

The prootic is well preserved on both sides of the braincase, showing details of its morphology. A large fossa containing two foramina lies ventral and caudal to a curved otosphenoidal crest. These foramina are separated from each other by an oblique septum and represent the exits of the maxillary and mandibular branches of the trigeminal nerve (V_{2-3}) and facial nerve (VII; Fig. 10). Two grooves come out of the foramen for the facial nerve, one extending rostroventrally and the other extending caudally (Fig. 10B), marking the courses of the rostral and caudal rami (palatine and hyomandibular nerves) of this nerve, respectively. Although the maxillomandibular and facial nerve foramina share a common fossa in the juvenile *Tarbosaurus bataar*, they are not united in a common external foramen in the braincase as they are in North American tyrannosaurids (Witmer and Ridgely, 2009). We regard the condition in MPC-D 107/7 as potentially representing the initial stage of an ontogenetic transformation that, with growth and thickening of the skull bones, results in the fossa transforming into more of a foramen. Our CT data on older specimens of *T. bataar* (e.g., MPC-D 107/14) corroborate this hypothetical ontogenetic sequence in that the maxillomandibular and facial nerve foramina reside within a shared bony space that is closer to a foramen in degree of enclosure, suggesting that derived tyrannosaurids indeed exhibit a fossa-to-foramen ontogenetic continuum. Finally, unlike in the adult *Tyrannosaurus rex* (Brochu, 2003; Witmer and Ridgely, 2009), there is no apparent prootic pneumatic fossa caudal to the foramen for V_{2-3}.

On the lateral aspect of the laterosphenoid ventral to the antotic crest lies a shallow depression, to which the dorsal end of the ascending process of the epipterygoid is attached (Fig. 10A). In this depression and medial to the epipterygoid lies a foramen through which the ophthalmic branch of the trigeminal nerve (V_1) would have exited the endocranial cavity, as described for *T. rex* by Molnar (1991), Brochu (2003), Holliday and Witmer (2008), and Witmer and Ridgely (2009). In addition, a foramen that may represent the exit of the oculomotor nerve (III) is present on the ventral part of the rostroventral surface of this bone (Fig. 10A).

The preserved portion of the parasphenoid includes the cultriform process and pituitary fossa (Figs. 4, 10A, C). Although the cultriform process is mediolaterally compressed and fractured, the CT data show that it is hollow inside as in *T. rex* (Brochu, 2003).

Among pneumatic sinuses, the rostral and caudal tympanic recesses have apertures open on the lateral aspect of the braincase (Fig. 10) as in larger individuals of *Tarbosaurus bataar* (e.g., MPC-D 107/14). The aperture of the rostral tympanic recess is dorsoventrally wide and opens caudal to the preotic pendant. The aperture of the caudal tympanic recess is large as in MPC-D 107/14, as well as in *T. rex* (Brochu, 2003; Witmer and Ridgely, 2009), and opens on the rostral aspect of the otoccipital and caudal to the columellar recess. Although tyrannosaurids apparently lack the dorsal tympanic recess (Witmer and Ridgely, 2009), the prootic of the present specimen bears a slight depression dorsal to the otosphenoidal crest (Fig. 10C).

Palatal Bones—The palate is mediolaterally compressed due to postmortem deformation, and its caudal part, especially on the right side, has mostly been weathered and is not preserved. The pterygoid is represented by the quadrate process, rostral part of the palatal plate, and rostrodorsal (vomerine) process of the left bone and rostrodorsal process of the right bone (Fig. 3). The rostrodorsal process expands dorsoventrally where it articulates with the palatine.

As mentioned above, the dorsal part of the right epipterygoid is preserved as attached to the laterosphenoid (Fig. 10A). The left epipterygoid is completely preserved in the matrix and still articulates with the quadrate process of the pterygoid as revealed by the CT data.

The preserved portion of the ectopterygoid includes the hook-like lateral process and adjacent part of the main body of the left bone, which is still mostly buried in the matrix (Figs. 2, 4A). The CT data revealed that these preserved parts are hollow inside.

The preserved, rostral part of the right palatine is exposed in right lateral view (Fig. 3) whereas a complete left bone is preserved within the matrix. The CT data showed that this bone is pneumatic as in other tyrannosaurids (e.g., Witmer, 1997; Brochu, 2003; Carr, 2010). On the left palatine, a very shallow depression lies on the lateral aspect of the rostral part of the maxillary process, followed caudally by two large fossae. Such fossae (Fig. 4A) are observed in mature individuals of *Tarbosaurus bataar* (e.g., Hurum and Sabath, 2003; MPC-D 107/2), as well as in most other large tyrannosaurids (Carr, 2010). The caudal fossa leads to a chamber that hollows out the vomeropterygoid (vomerine) process. The rostral projection of the vomeropterygoid process is relatively longer in the present specimen than in mature individuals (e.g., Hurum and Sabath, 2003; MPC-D 107/2). The maxillary process, which bears a deep groove for articulation with the maxilla on the lateral surface as exposed on the right side, is also apparently longer in the present specimen (Fig. 3) than in larger individuals.

The CT data revealed that the left and right vomers are already fused rostrally, whereas they appear to be separate from each other in the caudal part as in adult individuals of *T. bataar* (Hurum and Sabath, 2003) and other tyrannosaurids (e.g., Molnar, 1991; Brochu, 2003; Currie, 2003a). Significantly, the rostral end of the vomer is narrow, displaying the primitive, lanceolate shape typical of more basal tyrannosauroids (Holtz, 2001; Currie et al., 2003; Li et al., 2010). Given that adult *T. bataar* have the typically tyrannosaurine, transversely expanded, diamond-shaped vomer (Hurum and Sabath, 2003), it would seem that dramatic ontogenetic change is possible in this bone.

Sclerotic Ring—The right sclerotic ring is exposed in right lateral view, whereas the CT data show that the left one is also preserved within the matrix (Figs. 3, 4). On the right side, 10 sclerotic ossicles are preserved in articulation, with the ventral part of the ring, which would probably have included three or four additional ossicles, missing (Fig. 11A). Hurum and Sabath (2003) reported that the sclerotic ring of a subadult specimen of *Tarbosaurus bataar* consists of 15 ossicles. Each sclerotic ossicle is weakly convex laterally and has a low median ridge (Fig. 11B). As in birds and non-avian dinosaurs (e.g., Curtis and Miller, 1938; Ostrom, 1961), most ossicles have one end above and the other end beneath the adjacent ossicles. On several ossicles, a slightly concave facet on which the adjacent ossicle overlaps is visible laterally (Fig. 11B). Among the preserved ossicles, two of them overlap the adjacent ossicles on each end. These ossicles, referred to as '+' or positive elements (Lemmrich, 1931), are located on the rostrodorsal and caudodorsal parts of the ring, respectively (Fig. 11A).

On the left side, CT data revealed that the sclerotic ring occupies approximately the upper two thirds of the orbit, with its ventral end almost coinciding with that of the ventral ramus of the postorbital (Fig. 4A). It follows that the eye of this juvenile would have occupied a significant portion of the orbit, unlike in adult individuals in which the space for the eye is restricted to the dorsal part of the orbit by a rostrally extending suborbital process of the postorbital.

Dentary—The dentary appears to be slender, relatively shallower dorsoventrally than that of adult individuals (Figs. 2–4), conforming to an ontogenetic trend of the increase in the relative depth of this bone in tyrannosaurids (Carr, 1999; Currie, 2003b). The ventral margin of this bone is almost straight caudal to the symphyseal region. In ventral view, the dentary becomes the thickest mediolaterally at the point where the straight ventral margin angled rostrodorsally near the symphyseal region.

At the rostral end of the dentary, numerous pits/neurovascular foramina with diameters up to a few millimeters cover the labial surface of the bone (Figs. 2, 3A). Caudal to this region, most such foramina are aligned in two, dorsal and ventral rows, with only a few foramina lying outside of these two rows. The dorsal row is located at about 7 to 8 mm from the dorsal margin of the bone. As described by Hurum and Sabath (2003), foramina in this row lie much closer to one another in the rostral part of the bone than in the more caudal part (Fig. 3A). The ventral row of neurovascular foramina lies at around 5 to 6 mm from the ventral margin of the dentary.

Splenial—The splenial, especially the part rostral to the splenial foramen, is rostrocaudally more elongated (Fig. 3) than those in larger specimens illustrated in Maleev (1974) and Hurum and Sabath (2003). The CT data revealed that the rostrodorsal margin of this bone has a pronounced 'lip' or step, as described in adult *Tarbosaurus bataar* by Hurum and Sabath (2003). The ventral border of the splenial foramen is barely closed (based on the CT data on the right splenial; this region on the left splenial is damaged). Currie and Dong (2001) suggested that the closure of this ventral border of the splenial foramen may be an ontogenetic feature in tyrannosaurids based on the observations that this border is open in a putatively juvenile individual (the holotype specimen of "*Shanshanosaurus huoyanshanensis*") as well as in some larger specimens of *T. bataar* (e.g., Maleev, 1974) but is closed in other specimens of this species (Hurum and Currie, 2000; Hurum and Sabath, 2003). The present observation that this border is closed in MPC-D 107/7, which is an individual comparable to the holotype of "*S. huoyanshanensis*" in size, suggests that this characteristic may be simply individually variable rather than being controlled ontogenetically.

Surangular—The preserved left surangular has a prominent caudal surangular foramen (Fig. 4A). The size of this foramen, however, is relatively smaller than those in other tyrannosaurids, as in adult specimens of *Tarbosaurus bataar* (Holtz, 2004). The surangular shelf is well developed dorsal to the caudal surangular foramen, extending horizontally without covering this foramen in lateral view, unlike in the specimen of *Tyrannosaurus rex* illustrated by Osborn (1912). The CT scan data revealed that the facet for the attachment of the jaw adductor muscle on the

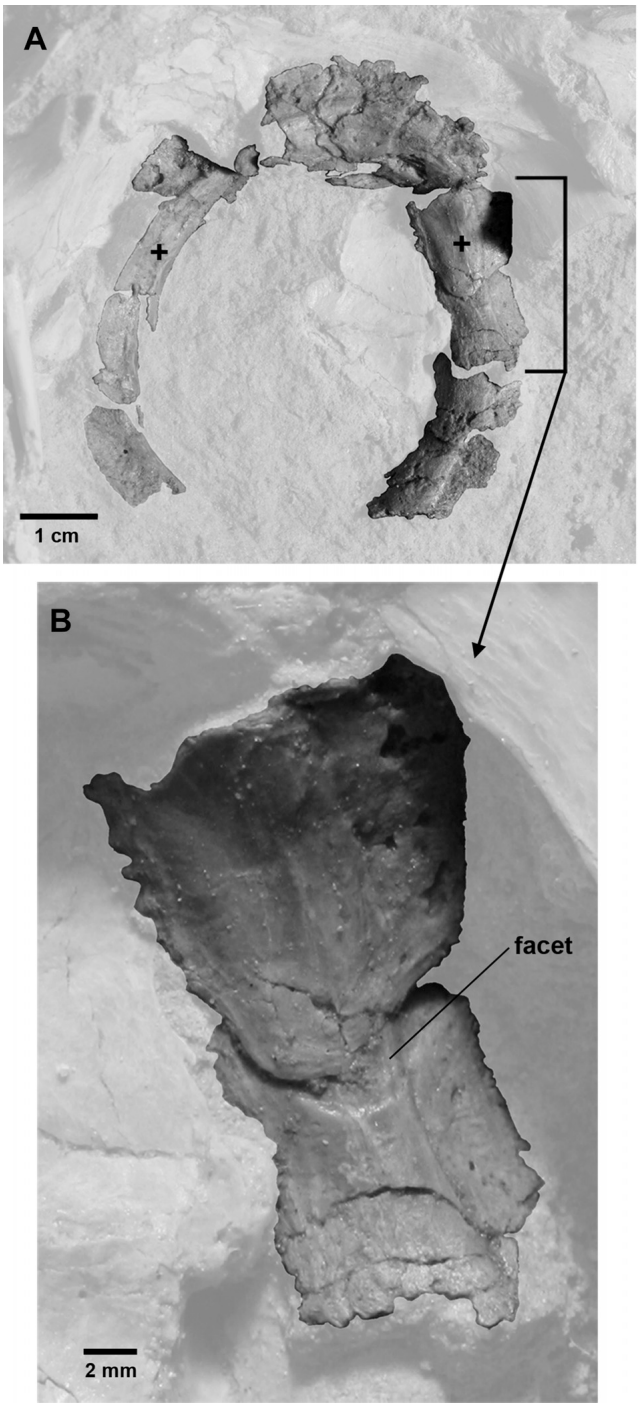

FIGURE 11. Right sclerotic ring of a juvenile *Tarbosaurus bataar* (MPC-D 107/7) in lateral view. **A**, entire preserved portion of the ring. Ossicles with '+' are those that overlap the adjacent ossicles on each end. **B**, close-up view of two ossicles showing a well-developed facet on one element on which the other element overlaps.

dorsal surface of the surangular shelf is slightly concave and faces dorsally. Unlike in *Alioramus altai* (Brusatte et al., 2009), there is no evidence of pneumatization of the surangular caudal to the caudal surangular foramen.

The articular is detached from the surangular and not preserved, suggesting that these two bones are not fused together, unlike in the adult condition of *T. bataar* described by Hurum and Currie (2000). With the caudal end of the prearticular broken off, the rugose surface for articulation with the articular and the hook-like process in front for contact with the articular and caudal part of the prearticular were exposed on the medial aspect of the surangular (Fig. 3A).

Other Bones of the Lower Jaw—Other mandibular bones are either only poorly preserved or morphologically very similar to adult conditions described in Hurum and Currie (2000) and Hurum and Sabath (2003). Based on the CT data, the supradentary and coronoid appear to be already fused to each other as in adult *Tarbosaurus bataar*. The left prearticular, partly exposed on the medial side of the left mandible (Fig. 3), shows that the bend between the caudal ramus and rostral ascending ramus is less acute than that in adults, which was described as "approximately perpendicular" by Hurum and Sabath (2003:186). The angular is preserved only on the left side. This bone is missing the rostral process that would have lied medial to the dentary. The preserved portion of this bone does not show much difference from those in larger individuals.

Dentition—The numbers of alveoli were confirmed based on the CT scan data. There are four alveoli both in the right and left premaxillae, 13 in the left maxilla, and 15 and 14 in the right and left dentaries, respectively (Fig. 6A). These are all within the known range of the numbers of alveoli in *Tarbosaurus bataar* (Maleev, 1974; Currie, 2003a, 2003b; Hurum and Sabath, 2003), suggesting that these are characteristics that do not change ontogenetically (Currie, 2003a, 2003b). The premaxillary teeth (Fig. 6B–D) have 'D-shaped' cross-sections typical of tyrannosaurids (e.g., Holtz, 2004). The maxillary and dentary teeth (Fig. 6E, F) are blade-like, labiolingually more flattened than those in larger individuals (Maleev, 1974; MPC-D 107/2). Among the preserved teeth on the left maxilla, the tooth crown height measured from the alveolar margin is the greatest on the third tooth (24.9 mm). All of the teeth in the left dentary and rostral five teeth in the right dentary are concealed by the maxillae. The CT images revealed that the fourth tooth is the longest among dentary teeth, both on the right and left sides.

All exposed teeth (left and right premaxillary, left maxillary, and right dentary teeth) are serrated. Therefore, an ontogenetic change of the first maxillary tooth from the unserrated to serrated conditions suggested for *Tyrannosaurus rex* by Carr and Williamson (2004) does not occur in *Tarbosaurus bataar*. The number of denticles per 5 mm varies among teeth, as demonstrated in *Tyrannosaurus rex* by Smith (2005). In each of the maxillary and dentary teeth for which the numbers of denticles were counted both on the mesial and distal carinae, densities of denticles are larger on the mesial carina than on the distal carina. In the six left maxillary teeth examined, densities of denticles range from 15.6 to 18.8 denticles per 5 mm on the mesial carina and from 13.3 to 16.3 denticles per 5 mm on the distal carina. In seven right dentary teeth, densities of denticles range from 19.8 to 24.7 denticles per 5 mm on the mesial carina and from 16.0 to 19.8 denticles per 5 mm on the distal carina. Because premaxillary teeth are packed tightly mesiodistally, the number of denticles could not be counted in most of these teeth, especially on the mesial carina. The density of denticles is 21.3 denticles per 5 mm on the mesial carina on the first tooth on the right side, the only premaxillary tooth for which this value could be examined, whereas such densities range from 16.2 to 17.4 denticles per 5 mm on the distal carinae in five premaxillary teeth (the third tooth on the left side and the second through fourth teeth on the right side).

DISCUSSION

Ontogenetic Changes in the Cranial Morphology

The present specimen, MPC-D 107/7, provides important new information on the ontogenetic changes in the cranial morphology of *Tarbosaurus bataar* in particular and Tyrannosauridae in general. The skull of MPC-D 107/7 is only slightly larger than that of the holotype specimen of "*Shanshanosaurus huoyanshanensis*" considered as a juvenile and the smallest-known *T. bataar* by Currie and Dong (2001) and is much more complete than the latter. MPC-D 107/7 thus increases the known growth range of various cranial bones in this dinosaur.

Most juvenile characteristics observed in MPC-D 107/7 are shared with those of North American tyrannosaurids detailed by Carr (1999), thus indicating that the ontogenetic changes in the cranial morphology are very similar between *T. bataar* and North American tyrannosaurids. One notable exception, however, is the proportion of the antorbital fenestra. An elongated antorbital fenestra was identified as a juvenile characteristic of tyrannosaurids by Carr (1999) and Carr and Williamson (2004). In MPC-D 107/7, however, the antorbital fenestra is only slightly longer than high (Fig. 2), and thus is not elongated rostrocaudally. This indicates that the shape of this fenestra does not change greatly in ontogeny of *T. bataar*, unlike that in North American tyrannosaurids.

To evaluate the ontogenetic stage of MPC-D 107/7 quantitatively, we added this specimen to Carr and Williamson's (2004) ontogenetic analysis on *Tyrannosaurus rex* (see Appendix 1 for coding of this specimen), as has previously been done for *Alioramus altai* by Brusatte et al. (2009). Obviously this procedure would work only if *T. bataar* followed an ontogenetic trajectory similar to that of *T. rex*. This assumption may be reasonable considering that *T. bataar* has been placed as the sister taxon of *T. rex* in past phylogenetic analyses (Holtz, 2001, 2004; Carr et al., 2005; Brusatte et al., 2009, 2010; Carr and Williamson, 2010; but see Currie et al., 2003, for a different view). In addition, *T. bataar* and *T. rex* are comparable in size (e.g., Holtz, 2004), and Bybee et al. (2006) demonstrated that theropods of similar maximum size followed nearly identical mass growth trajectories. We ran an analysis with the 'artificial adult' removed from the original data matrix in Carr and Williamson (2004) using PAUP* 4.0b10 (Swofford, 2002) under a branch-and-bound search. This analysis resulted in two most parsimonious trees, which have a tree length of 98 and, excluding uninformative characters, have a consistency index of 0.94, homoplasy index of 0.06, retention index of 0.97, and rescaled consistency index of 0.91. These two trees are different only in the relative positions of MPC-D 107/7 and CMNH 7541, holotype specimen of *Nanotyrannus lancensis*. That is, MPC-D 107/7 is placed at a younger growth stage than CMNH 7541 in one tree, and vice versa in the other (Fig. 12A). Incongruent distributions of certain character states (presence/absence and morphology of the frontal sagittal crest and shapes of the antorbital fenestra, orbital margin of the jugal, and dentary) contributed to this equivocal positioning of these two specimens. That is, MPC-D107/7 lacks the frontal sagittal crest (state 0 of characters 57 and 58) and retains a dorsoventrally shallow dentary (state 0 of character 81) as in the hypothetical 'embryo,' but has a round antorbital fenestra and a concave orbital margin of the jugal (state 1 of characters 28 and 43, respectively) as in individuals of more advanced growth stages. In contrast, CMNH 7541 has an elongated antorbital fenestra and a straight orbital margin of the jugal (state 0 of characters 28 and 43, respectively) as hypothesized to be present in the hypothetical 'embryo,' but has already acquired the frontal sagittal crest (state 1 of characters 57 and 58) and a deep dentary (state 1 of character 81) as in individuals of more advanced growth stages. These incongruent character states may be due to difference in the ontogenetic trajectory between *T. bataar* and *T. rex*. For example, the shape of the antorbital

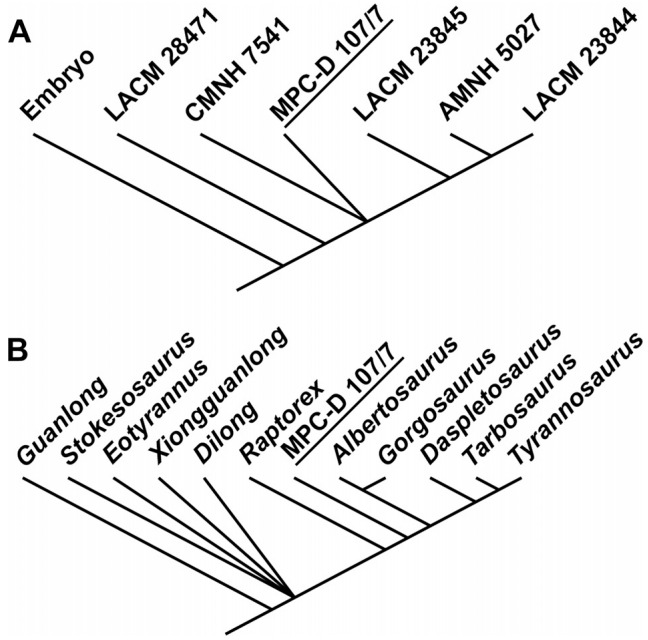

FIGURE 12. Results of cladistic analyses based on published data matrices with addition of MPC-D 107/7. **A**, strict consensus of two most parsimonious trees resulting from the ontogenetic analysis based on the data matrix of Carr and Williamson (2004). **B**, strict consensus of 140 most parsimonious trees resulting from the phylogenetic analysis based on the data matrix of Sereno et al. (2009).

fenestra may not change drastically during ontogeny in *T. bataar*, unlike in *T. rex*, as suggested above. Nonetheless, this result confirms a very young ontogenetic status of MPC-D107/7, emphasizing the fact that this specimen is among the youngest and most complete skulls known for tyrannosaurids.

It has been suggested that adult tyrannosaurid skulls have high bending and torsional strength (e.g., Holtz, 2003; Snively et al., 2006). This is especially the case with adult *T. bataar* and *T. rex*, in which the articulation between the nasal and maxilla is reinforced by the interdigitating suture consisting of transverse ridges and grooves. In addition, Rayfield (2004) suggested that the rugose nasals and the postorbitals with thickened cornual processes of tyrannosaurids are adapted for resisting compressive and shearing stresses that are concentrated on these bones. Together with mediolaterally thick lateral teeth (e.g., Farlow et al., 1991; Holtz, 2003) and rigid lower jaws (Hurum and Currie, 2000), these aspects of morphology suggest that adult tyrannosaurids were well adapted for resisting high stress and strain resulting from engaging large prey (e.g., Snively et al., 2006). The skull of MPC-D 107/7 demonstrates that the skull of the juvenile *T. bataar* lacks some of the morphological characteristics that are adapted for bearing great feeding forces. Firstly, the dorsal surfaces of the nasals are smooth and the postorbital lacks a cornual process in the juvenile *T. bataar.* In addition, bones such as the maxilla are relatively thinner mediolaterally in the juvenile skull than in adult individuals, suggesting that these bones in the former would have been weaker against stress and strain (especially transversely) than in the latter. Secondly, as exemplified by a dorsoventrally low maxilla (Fig. 7B), the dorsoventral height of the juvenile skull is relatively smaller that that of adult skulls, suggesting that the juvenile skull is weaker in dorsoventral bending than adult skulls (Snively et al., 2006). Thirdly, vaulting of the nasals, which contributes to increasing strength in bending and torsion (Snively et al., 2006), is much less pronounced in the juvenile *T. bataar* than in adult individuals. In addition, the suture between the nasal and maxilla in the juvenile skull consists of a longitudinal groove and lacks interdigitating transverse ridges and grooves that reinforce this suture in adult individuals as mentioned by Snively et al. (2006). Furthermore, lateral teeth of the juvenile *T. bataar* are relatively thinner labiolingually than those in adults (Fig. 6E, F) and thus have less labiolingual bending strength than the latter. These observations suggest that during ontogeny *T. bataar* would have changed its dietary niches, as has been suggested for tyrannosaurids in general (Molnar and Farlow 1990; Snively et al., 2006).

Implications for Tyrannosauroid Taxonomy

The present specimen sheds light on several issues in tyrannosauroid taxonomy, albeit indirectly. First, one contentious issue in this field is the status of the North American *Nanotyrannus lancensis*, whether it is a distinct taxon or represents a young individual of the coeval *Tyrannosaurus rex*. In his detailed analysis, Carr (1999) demonstrated that the holotype of *N. lancensis* (CMNH 7541) is an immature individual and further suggested that it pertains to a juvenile *T. rex* by proposing numerous cranial characteristics as being shared between CMNH 7541 and specimens of *T. rex.* Currie (2003a), however, argued that almost all such characters proposed by Carr (1999) are not restricted to CMNH 7541 and *T. rex* but are more broadly distributed in Tyrannosauridae. This demonstrates that a consensus has not been reached on this issue, with some recent studies regarding CMNH 7541 as a juvenile *T. rex* (e.g., Holtz, 2001, 2004; Carr and Williamson, 2004; Brusatte et al., 2009, 2010), whereas others considering it as representing a distinct taxon (e.g., Currie et al., 2003; Larson, 2008).

One focal point of this issue relates to tooth counts. The holotype of *N. lancensis* has 14 or 15 maxillary teeth (Gilmore, 1946; Bakker et al., 1988), whereas *T. rex* has 11 or 12 maxillary teeth (e.g., Currie, 2003a, 2003b; Smith, 2005). Likewise, Witmer and Ridgely (2010) reported 16 dentary tooth positions in CMNH 7541 (based on the CT scan data), whereas definitive adult *T. rex* has 11–14 dentary teeth (Hurum and Sabath, 2003; Holtz, 2004; Smith, 2005). Carr (1999) suggested that the number of maxillary alveoli decreases ontogenetically in tyrannosaurids based on his observations on *Gorgosaurus libratus*, implying that the high count of the alveoli in CMNH 7541 is a juvenile characteristic that would have decreased later in ontogeny. Currie (2003a, 2003b), on the other hand, found no clear ontogenetic trends (neither decrease nor increase) in the number of the maxillary teeth in any tyrannosaurids he examined, including *G. libratus*.

Data on MPC-D 107/7 may contribute to clarifying such ontogenetic trends. Currie (2003a, 2003b) examined specimens of *T. bataar*, of which length of the maxillary tooth row ranges from approximately 200 mm to approximately 600 mm, and found that those specimens have either 12 or 13 maxillary teeth with no apparent trend in ontogenetic changes. In MPC-D 107/7, the left maxilla has the tooth row length of 137 mm and bears 13 alveoli. Likewise, the 14–15 dentary tooth positions we observe in MPC-D 107/7 agrees exactly with the range in adult *T. bataar* as reported by Hurum and Sabath (2003). Therefore, numbers of alveoli in this specimen, being a much smaller (and presumably younger) individual than those examined in Currie (2003a, 2003b), are consistent with the latter author's finding that there is no tendency for reduction of numbers of maxillary alveoli in tyrannosaurids, and cast doubt on Carr's (1999) hypothesis that the high numbers of the maxillary teeth observed in CMNH 7541 would have decreased later in ontogeny to those seen in *T. rex*, especially considering that CMNH 7541 with a skull length of 572 mm is already a much larger and presumably considerably older individual than MPC-D 107/7. It is noteworthy, however, that data in both Carr (1999) and Currie (2003a, 2003b) show that

there is individual, non-ontogenetic variation in maxillary tooth counts in tyrannosaurids. Therefore, more specimens comparable to MPC-D 107/7 in ontogenetic stage would be necessary to confirm apparently constant numbers of alveoli during ontogeny of *T. bataar* and other tyrannosaurids.

The second issue relates to the significance of presence/absence of a pneumatic foramen within the concavity of the dorsal ramus of the quadratojugal. Both CMNH 7541 and another small tyrannosaurid specimen from the Maastrichtian of North America, BMR P2002.4.1, possess such a pneumatic foramen (Witmer and Ridgely, 2010), but it is absent in adult specimens of definitive *T. rex*. Thus, if CMNH 7541 and BMR P2002.4.1 are regarded as juvenile *T. rex*, one must argue for ontogenetic loss of the foramen. The absence of the foramen in MPC-D 107/7 and adult *T. bataar* specimens shows that this species underwent no such ontogenetic transformation. *Tyrannosaurus rex* may have gone through such a unique transformation or, again, the foramen may be an individual variant, but MPC-D 107/7 shows that this ontogeny was not typical for tyrannosaurids.

The third issue is taxonomic assignment of the holotype specimen of "*Shanshanosaurus huoyanshanensis*." Between coeval *Tarbosaurus* and *Alioramus*, Currie and Dong (2001) concluded that this specimen more likely pertains to the former. Information on MPC-D 107/7 supports this conclusion. Firstly, the caudal surangular foramen of "*S. huoyanshanensis*" appears to be small, as is the one in MPC-D 107/7. A small size of this foramen is considered as a characteristic of *T. bataar* (Holtz, 2004). In contrast, this foramen in *Alioramus remotus* and *Alioramus altai* is large (Kurzanov, 1976; Brusatte et al., 2009). Secondly, the maxilla of the "*S. huoyanshanensis*" is dorsoventrally deeper than that of *A. altai* (this bone of *A. remotus* is not completely preserved). On the other hand, the height-to-length ratios of the maxillae are very similar between "*S. huoyanshanensis*" and MPC-D 107/7 (75 mm in height vs. 180 mm in length in the former [Currie and Dong, 2001] and 78 mm in height vs. 187 mm in length in the latter). These similarities between "*S. huoyanshanensis*" and MPC-D 107/7 suggest that the former most likely belongs to *T. bataar* among coeval, Asian tyrannosaurids.

Finally, Sereno et al. (2009) recently described a new tyrannosauroid, *Raptorex kriegsteini*, reportedly from the Lower Cretaceous of China and regarded it as the sister taxon to Tyrannosauridae. *Raptorex* looks at first glance remarkably like MPC-D 107/7, and consequently we compare the two here. Excluding one character (character 61) that was miscoded for *R. kriegsteini* in Sereno et al.'s (2009) data matrix, plesiomorphic character states of 10 cranial and three postcranial characters unambiguously supported the phylogenetic position of this species outside of Tyrannosauridae in their phylogenetic analysis. Among these 10 cranial, plesiomorphic character states, seven (state 0 for characters 2, 4, 29, 30, 54, and 62 and state 1 for character 6) are shared with MPC-D 107/7, affirming the findings of others (e.g., Carr, 1999; Brusatte et al., 2009) that discriminating juvenile characters from plesiomorphic characters can be challenging without additional criteria. For example, two such character states, the smooth dorsal surface and absence of the suborbital flange of the postorbital (coded as the plesiomorphic state 0 for characters 29 and 30, respectively, by Sereno et al., 2009), were identified as juvenile characteristics of tyrannosaurids by Carr (1999) and Carr and Williamson (2004). In addition, two of the characteristics that Sereno et al. (2009) proposed as diagnostic of *R. kriegsteini*, a shallow suborbital part of the jugal and presence of an accessory pneumatic fossa dorsal to the maxillary fenestra within the antorbital fossa, are also observed in MPC-D 107/7 (Fig. 2) as described above, again confounding the unambiguous assessment of characters as being primitive, derived, juvenile, or adult.

To test the effects of potentially juvenile characteristics on the phylogenetic hypothesis, we added MPC-D 107/7 in Sereno et al.'s (2009) data matrix for tyrannosauroid phylogeny (see Appendix 2 for coding of this specimen) and ran an analysis using PAUP* 4.0b10 (Swofford, 2002) under a branch-and-bound search. This analysis resulted in 140 most parsimonious trees, which have a tree length of 127, consistency index of 0.83, homoplasy index of 0.17, retention index of 0.94, and rescaled consistency index of 0.79. The strict consensus of these 140 trees shows the same branching pattern within Tyrannosauroidea as the one obtained by Sereno et al. (2009:fig. 4) except for the addition of MPC-D 107/7 as the sister taxon to Tyrannosauridae (Fig. 12B). This result therefore confirms that a juvenile tyrannosaurid would be placed at a much more basal position than an adult of the same species in the phylogenetic analysis, and opens up the possibility that *R. kriegsteini* may be a juvenile of a more derived tyrannosaurid. Sereno et al. (2009) concluded that the holotype specimen of *R. kriegsteini* is a subadult or young adult nearing mature body size based on several skeletal features, despite the fact that its estimated age of death is 5 to 6 years old and thus is fairly young. If Sereno et al.'s (2009) conclusion is accepted, it follows that the holotype specimen of *R. kriegsteini* already shows matured cranial morphology of this species and that such morphology is recapitulated in juveniles of derived tyrannosaurids as observed in MPC-D 107/7.

Further scrutiny of *R. kriegsteini* is thus warranted to decide on whether it is a juvenile tyrannosaurid or a more basally positioned taxon. That said, comparison of MPC-D 107/7 and *R. kriegsteini*, which have similar skull lengths (290 mm and 300 mm, respectively), suggests that the latter may not pertain to a juvenile *T. bataar*. Several details of skull morphology appear to be different between *R. kriegsteini* and MPC-D 107/7. For example, the rostroventral lamina of the ventral ramus of the lacrimal onto which the antorbital fossa extends is dorsoventrally much taller in *R. kriegsteini* than in MPC-D 107/7. In addition, the caudal surangular foramen is relatively large in *R. kriegsteini* compared to those in both juvenile and adult *T. bataar* (S. Brusatte, pers. comm.). Whereas a possibility that these differences in cranial features representing intraspecific variation cannot be completely excluded, there is also one postcranial feature that distinguishes *R. kriegsteini* from MPC-D 107/7, and in fact, from all other tyrannosauroids. That is, the ilium of *R. kriegsteini* is reported to lack a vertical crest dorsal to the acetabulum on the lateral surface (Sereno et al., 2009). The presence of such a crest is a tyrannosauroid synapomorphy (e.g., Holtz, 2001, 2004), and MPC-D 107/7 does possess this characteristic. Accordingly, we tentatively conclude that, in accordance with its reportedly very different stratigraphic age and provenance, *R. kriegsteini* is not a juvenile *T. bataar*. Perhaps of greater general significance, the impact of MPC-D 107/7 on debates surrounding the status of *R. kriegsteini*, "*S. huoyanshanensis*," and CMNH 7541 highlights the potential difficulties in discriminating plesiomorphic from juvenile characters and the importance of taxonomically unambiguous juvenile specimens such as MPC-D 107/7

ACKNOWLEDGMENTS

We are grateful to K. Hayashibara (former president of the Hayashibara Company Limited, Okayama, Japan) for his continuous financial support to the Japanese-Mongolian Joint Paleontological Expedition since 1993. Thanks are also due to the Japanese (Hayashibara Museum of Natural Sciences) and Mongolian (MPC) members of the joint expedition team for their help in the field and laboratories. We thank H. Rockhold, RT, and O'Bleness Memorial Hospital, in Athens, Ohio, for help with CT scanning and T. Hieronymus for his advice on preparation on histological thin sections. The drawing in Figure 2 was skillfully executed by U. Kikutani. Olympus, Mitsubishi Motor Company, and Panasonic supported the expedition. T.T. thanks M. Manabe (National Museum of Nature and Science, Tokyo) for continuous support for his research.

T.T. was supported by JSPS Postdoctoral Fellowships, JSPS Postdoctoral Fellowships for Research Abroad, and Grant-in-Aid for JSPS Fellows from the Japan Society for Promotion of Science. L.M.W.'s and R.C.R.'s work was supported by NSF IBN-0343744 and IOB-0517257. Editor H.-D. Sues, S. Brusatte, and an anonymous reviewer made constructive suggestions that improved the clarity of the manuscript. Translations of Russian papers were obtained courtesy of the Polygot Paleontologists website (http://www.paleoglot.org).

LITERATURE CITED

Bakker, R.T., M. Williams, and P. J. Currie. 1988. *Nanotyrannus*, a new genus of pygmy tyrannosaur, from the latest Cretaceous of Montana. Hunteria 1(5):1–30.

Barsbold, R. 1974. Saurornithoididae, a new family of small theropod dinosaurs from central Asia and North America. Palaeontologia Polonica 30:5–22.

Barsbold, R. 1983. [Carnivorous dinosaurs from the Cretaceous of Mongolia]. Trudy, Sovmestnaya Sovietsko-Mongol'skaya Paleontologicheskaya Ekspeditsiya 19:1–117. [Russian]

Brochu, C. A. 2003. Osteology of *Tyrannosaurus rex*: insights from a nearly complete skeleton and high-resolution computed tomographic analysis of the skull. Society of Vertebrate Paleontology Memoir 7:1–138.

Brusatte, S. L., T. D. Carr, G. M. Erickson, G. S. Bever, and M. A. Norell. 2009. A long-snouted, multihorned tyrannosaurid from the Late Cretaceous of Mongolia. Proceedings of the National Academy of Sciences of the United States of America 106:17261–17266.

Brusatte, S. L., M. A. Norell, T. D. Carr, G. M. Erickson, J. R. Hutchinson, A. M. Balanoff, G. S. Bever, J. N. Choiniere, P. J. Makovicky, and X. Xu. 2010. Tyrannosaur paleobiology: new research on ancient exemplar organisms. Science 329:1481–1485.

Bybee, P. J., A. H. Lee, and E.-T. Lamm. 2006. Sizing the Jurassic theropod dinosaur *Allosaurus*: assessing growth strategy and evolution of ontogenetic scaling of limbs. Journal of Morphology 267:347–359.

Carr, T. D. 1999. Craniofacial ontogeny in Tyrannosauridae (Dinosauria, Coelurosauria). Journal of Vertebrate Paleontology 19:497–520.

Carr, T. D. 2005. Phylogeny of Tyrannosauroidea (Dinosauria: Coelurosauria) with special reference to North American forms. Ph.D. dissertation, University of Toronto, Toronto, Ontario, Canada, 1170 pp.

Carr, T. D. 2010. A taxonomic assessment of the type series of *Albertosaurus sarcophagus* and the identity of Tyrannosauridae (Dinosauria, Coelurosauria) in the *Albertosaurus* bonebed from the Horseshoe Canyon Formation (Campanian–Maastrichtian, Late Cretaceous). Canadian Journal of Earth Sciences 47:1213–1226.

Carr, T. D., and T. E. Williamson. 2004. Diversity of late Maastrichtian Tyrannosauridae (Dinosauria: Theropoda) from western North America. Zoological Journal of the Linnean Society 142:479–523.

Carr, T. D., and T. E. Williamson. 2010. *Bistahieversor sealeyi*, gen. et sp. nov., a new tyrannosauroid from New Mexico and the origin of deep snouts in Tyrannosauroidea. Journal of Vertebrate Paleontology 30:1–16.

Carr, T. D., T. E. Williamson, and D. R. Schwimmer. 2005. A new genus and species of tyrannosauroid from the Late Cretaceous (middle Campanian) Demopolis Formation of Alabama. Journal of Vertebrate Paleontology 25:119–143.

Cooper, L. N., A. H. Lee, M. L. Taper, and J. R. Horner. 2008. Relative growth rates of predator and prey dinosaurs reflect effects of predation. Proceedings of the Royal Society B 275:2609–2615.

Currie, P. J. 2000. Theropods from the Cretaceous of Mongolia; pp. 434–455 in M. J. Benton, M. A. Shishkin, D. M. Unwin, and E. N. Kurochkin (eds.), The Age of Dinosaurs in Russia and Mongolia. Cambridge University Press, Cambridge, U.K.

Currie, P. J. 2003a. Cranial anatomy of tyrannosaurid dinosaurs from the Late Cretaceous of Alberta, Canada. Acta Palaeontologica Polonica 48:191–226.

Currie, P. J. 2003b. Allometric growth in tyrannosaurids (Dinosauria: Theropoda) from the Upper Cretaceous of North America and Asia. Canadian Journal of Earth Sciences 40:651–665.

Currie, P. J., and K. Carpenter. 2000. A new specimen of *Acrocanthosaurus atokensis* (Dinosauria: Theropoda) from the Lower Cretaceous Antlers Formation (Lower Cretaceous, Aptian) of Oklahoma, USA. Geodiversitas 22:207–246.

Currie, P. J., and Z.-M. Dong. 2001. New information on *Shanshanosaurus huoyanshanensis*, a juvenile tyrannosaurid (Theropoda, Dinosauria) from the Late Cretaceous of China. Canadian Journal of Earth Sciences 38:1729–1737.

Currie, P. J., J. H. Hurum, and K. Sabath. 2003. Skull structure and evolution in tyrannosaurid dinosaurs. Acta Palaeontologica Polonica 48:227–234.

Curtis, E. L., and R. C. Miller. 1938. The sclerotic ring in North American birds. Auk 55:225–243.

Dong, Z.-M. 1977. [On the dinosaurian remains from Turpan, Xinjiang]. Vertebrata PalAsiatica 15:59–66. [Chinese]

Erickson, G. M., P. J. Makovicky, P. J. Currie, M. A. Norell, S. A. Yerby, and C. A. Brochu. 2004. Gigantism and comparative life-history parameters of tyrannosaurid dinosaurs. Nature 430:772–775.

Farlow, J. M., D. L. Brinkma, W. L. Abler, and P. J. Currie. 1991. Size, shape, and serration density of theropod dinosaur lateral teeth. Modern Geology 16:161–198.

Gilmore, C. W. 1946. A new carnivorous dinosaur from the Lance Formation of Montana. Smithsonian Miscellaneous Collections 106:1–19.

Gradzínski, R., Z. Kielen-Jaworowska, and T. Maryańska. 1977. Upper Cretaceous Djadokhta, Barun Goyot and Nemegt formations of Mongolia, including remarks on previous subdivisions. Acta Geologica Polonica 27:281–317.

Holliday, C. M., and L. M. Witmer. 2008. Cranial kinesis in dinosaurs: intracranial joints, protractor muscles, and their significance for cranial evolution and function in diapsids. Journal of Vertebrate Paleontology 28:1073–1088.

Holtz, T. R., Jr. 2001. The phylogeny and taxonomy of the Tyrannosauridae; pp. 64–83 in D. H. Tanke and K. Carpenter (eds.), Mesozoic Vertebrate Life. Indiana University Press, Bloomington, Indiana.

Holtz, T. R., Jr. 2003. Dinosaur predation: evidence and ecomorphology; pp. 325–340 in P. H. Kelly, M. Kowalewski, and T. A. Hansen (eds.), Predator-Prey Interactions in the Fossil Record. Topics in Geobiology, Volume 20. Kluwer Academic/Plenum Publishers, New York, New York.

Holtz, T. R., Jr. 2004. Tyrannosauroidea; pp. 111–136 in D. B. Weishampel, P. Dodson, and H. Osmólska (eds), The Dinosauria, second edition. University of California Press, Berkeley, California.

Horner, J. R., and K. Padian. 2004. Age and growth dynamics of *Tyrannosaurus rex*. Proceedings of the Royal Society of London B 271:1875–1880.

Huene, F. von. 1914. Das natürliche System der Saurischia. Centralblatt für Mineralogie, Geologie und Palaöntologie Jahrgang Abteilung B 1914:154–158.

Hurum, J. H., and P. J. Currie. 2000. The crushing bite of tyrannosaurids. Journal of Vertebrate Paleontology 20:619–621.

Hurum, J. H., and K. Sabath. 2003. Giant theropod dinosaurs from Asia and North America: skulls of *Tarbosaurus bataar* and *Tyrannosaurus rex* compared. Acta Palaeontologica Polonica 48:161–190.

Jerzykiewicz, T. 2000. Lithostratigraphy and sedimentary settings of the Cretaceous dinosaur beds of Mongolia; pp. 279–296 in M. J. Benton, M. A. Shishkin, D. M. Unwin, and E. N. Kurochkin (eds.), The Age of Dinosaurs in Russia and Mongolia. Cambridge University Press, Cambridge, U.K.

Jerzykiewicz, T., and D. A. Russell. 1991. Late Mesozoic stratigraphy and vertebrates of the Gobi Basin. Cretaceous Research 12:345–377.

Kurochkin, E. N., and R. Barsbold. 2000. The Russian-Mongolian expeditions and research in vertebrate paleontology; pp. 235–255 in M. J. Benton, M. A. Shishkin, D. M. Unwin, and E. N. Kurochkin (eds.), The Age of Dinosaurs in Russia and Mongolia. Cambridge University Press, Cambridge, U.K.

Kurzanov, S. M. 1976. [A new late Cretaceous carnosaur from Nogon-Tsav, Mongolia.] Sovmestnaya Sovietsko-Mongol'skaya Paleontologicheskaya Ekspeditsiya 3:93–104. [Russian]

Larson, P. 2008. Variation and sexual dimorphism in *Tyrannosaurus rex*; pp. 102–128 in P. Larson and K. Carpenter (eds.), *Tyrannosaurus rex*, The Tyrant King. Indiana University Press, Bloomington, Indiana.

Lemmrich, W. 1931. Der Skleralring der Vögel. Jenaische Zeitschrift für Naturwissenschaften 65:513–586.

Li, D., M. A. Norell, K.-Q. Gao, N. D. Smith, and P. J. Makovicky. 2010. A longirostrine tyrannosauroid from the Early Cretaceous of China. Proceedings of the Royal Society B 277:183–190.

Maleev, E. A. 1955a. [A gigantic carnivorous dinosaur of Mongolia]. Doklady Akademii Nauk SSSR 104:634–637. [Russian]
Maleev, E. A. 1955b. [New carnivorous dinosaurs from the Upper Cretaceous of Mongolia]. Doklady Akademii Nauk SSSR 104:779–783. [Russian]
Maleev, E. A. 1965. [The carnosaur dinosaur brain.] Paleontologicheskii Zhurnal 1965:141–143. [Russian]
Maleev, E. A. 1974. [Gigantic carnosaurs of the family Tyrannosauridae]. Trudy, Sovmestnaya Sovietsko-Mongol'skaya Paleontologicheskaya Ekspeditsiya 1:132–191. [Russian]
Marsh, O. C. 1881. Classification of the Dinosauria. American Journal of Science (series 3) 23:81–86.
Molnar, R. E. 1991. The cranial morphology of *Tyrannosaurus rex*. Palaeontographica A 217:137–176.
Molnar, R. E., and J. O. Farlow. 1990. Carnosaur paleobiology; pp. 210–224 in D. B. Weishampel, P. Dodson, and H. Osmólska (eds), The Dinosauria. University of California Press, Berkeley, California.
Osborn, H. F. 1906. *Tyrannosaurus*, Upper Cretaceous carnivorous dinosaur (second communication). Bulletin of the American Museum of Natural History 22:281–296.
Osborn, H. F. 1912. Crania of *Tyrannosaurus* and *Allosaurus*. Memoirs of the American Museum of Natural History (New series) 1:1–30.
Ostrom, J. H. 1961. Cranial morphology of the hadrosaurian dinosaurs of North America. Bulletin of the American Museum of Natural History 122:33–186.
Owen, R. 1842. Report on British fossil reptiles. Part II. Report of the British Association for the Advancement of Science 11:60–204.
Rayfield, E. J. 2004. Cranial mechanics and feeding in *Tyrannosaurus rex*. Proceedings of the Royal Society of London B 271:1451–1459.
Rozhdestvensky, A. K. 1965. [Growth changes in Asian dinosaurs and some problems of their taxonomy]. Paleontologicheskii Zhurnal 1965:95–100. [Russian]
Sampson, S. D., and L. M. Witmer. 2007. Craniofacial anatomy of *Majungasaurus crenatissimus* (Theropoda: Abelisauridae) from the Late Cretaceous of Madagascar. Society of Vertebrate Paleontology Memoir 8:32–102.
Saveliev, S., and V. Alifanov 2007. A new study of the brain of the predatory dinosaur *Tarbosaurus bataar* (Theropoda, Tyrannosauridae). Paleontological Journal 41:281–289.
Sereno, P. C., L. Tan, S. L. Brusatte, H. J. Kriegstein, X. Zhao, and K. Cloward. 2009. Tyrannosaurid skeletal design first evolved at small body size. Science 326:418–422.
Shuvalov, V. F. 2000. The Cretaceous stratigraphy and paleobiogeography of Mongolia; pp. 256–278 in M. J. Benton, M. A. Shishkin, D. M. Unwin, and E. N. Kurochkin (eds.), The Age of Dinosaurs in Russia and Mongolia. Cambridge University Press, Cambridge, U.K.
Smith, J. B. 2005. Heterodonty in *Tyrannosaurus rex*: implications for the taxonomic and systematic utility of theropod dentitions. Journal of Vertebrate Paleontology 25:865–887.
Snively, E., D. M. Henderson, and D. S. Phillips. 2006. Fused and vaulted nasals of tyrannosaurid dinosaurs: implications for cranial strength and feeding mechanics. Acta Palaeontologica Polonica 51:435–454.
Suzuki, S., and M. Watabe. 2000. Report on the Japan-Mongolia Joint Paleontological Expedition to the Gobi Desert, 1995. Hayashibara Museum of Natural Sciences Research Bulletin 1:45–57.
Swofford, D. L. 2002. PAUP*: Phylogenetic Analysis Using Parsimony (*And Other Methods). Version 4. Sinauer Associates, Sunderland, Massachusetts.
Tsuihiji, T. 2010. Reconstructions of the axial muscle insertions in the occipital region of dinosaurs: evaluations of past hypotheses on Marginocephalia and Tyrannosauridae using the Extant Phylogenetic Bracket approach. Anatomical Record 293:1360–1386.
Watabe, M., and S. Suzuki. 2000a. Cretaceous fossil localities and a list of fossils collected by Hayashibara Museum of Natural Sciences and Mongolian Paleontological Center Joint Paleontological Expedition (JMJPE) from 1993 through 1998. Hayashibara Museum of Natural Sciences Research Bulletin 1:99–108.
Watabe, M., and S. Suzuki. 2000b. Report on the Japan-Mongolia Joint Paleontological Expedition to the Gobi Desert, 1994. Hayashibara Museum of Natural Sciences Research Bulletin 1:30–44.
Weishampel, D. B., D. E. Fastovsky, M. Watabe, D. Varricchio, F. Jackson, K. Tsogtbaatar, and R. Barsbold. 2008. New oviraptorid embryos from Bugin-Tsav, Nemegt Formation (Upper Cretaceous), Mongolia, with insights into their habitat and growth. Journal of Vertebrate Paleontology 28:1110–1119.
Witmer, L. M. 1997. The evolution of the antorbital cavity of archosaurs: a study in soft-tissue reconstruction in the fossil record with an analysis of the function of pneumaticity. Society of Vertebrate Paleontology Memoir 3:1–73.
Witmer, L. M., and R. C. Ridgely. 2008. The paranasal air sinuses of predatory and armored dinosaurs (Archosauria: Theropoda and Ankylosauria) and their contribution to cephalic architecture. Anatomical Record 291:1362–1388.
Witmer, L. M., and R. C. Ridgely. 2009. New insights into the brain, braincase, and ear region of tyrannosaurs (Dinosauria, Theropoda), with implications for sensory organization and behavior. Anatomical Record 292:1266–1296.
Witmer, L. M., and R. C. Ridgely. 2010. The Cleveland tyrannosaur skull (*Nanotyrannus* or *Tyrannosaurus*): new findings based on CT scanning, with special reference to the braincase. Kirtlandia 51:61–81.

Submitted July 9, 2010; accepted January 12, 2011.
Handling editor: Hans-Dieter Sues.

APPENDIX 1. Character state values of MPC-D107/7 for the 84 characters in the data matrix by Carr and Williamson (2004) coded in the present ontogenetic analysis.

```
0000000000 00?011000? 00000001?? ?0000??000
0010000000 00100?0000 00000?00?1 ?00000?00?
0000
```

APPENDIX 2. Character state values of MPC-D107/7 for the 101 characters in the data matrix by Sereno et al. (2009) coded in the present phylogenetic analysis.

```
10101101?1 0000010O?1 000000?000 0111110012
1?10001??? 1110?1111? 2010111011 1111111110
11111111?1 1111111111 1
```